One-Loop MSSM predictions for $B_{s,d} \rightarrow \ell^+\ell^-$atlowtan$\beta$

Philip Tanedo

One-Loop MSSM Predictions for $B_{s,d} \to \ell^+ \ell'^-$ at low $\tan\beta$

A thesis presented for the degree of
Master of Science by Research

by

Philip Tanedo

April 2009

Institute for Particle Physics Phenomenology

Durham University

Abstract

One of the most promising signals of new physics at colliders is the rare decay $B_s^0 \to \mu^+ \mu^-$. The LHC will be the first experiment to directly probe this loop- and helicity- suppressed decay channel down to the Standard Model prediction. Deviations from the predicted branching ratio are a signature of new particles in the loops. In particular, it is well known that the MSSM prediction scales as $\tan^6 \beta$ due to the supersymmetric Higgs penguin diagrams, making this a fertile testing-ground for SUSY. In this study we analyse the MSSM prediction for the general process $B_{s,d} \to \ell^+ \ell'^-$ in the hertofore unexplored low tan beta region of the MSSM parameter space where interference with the box and Z-penguin diagrams could cause the branching ratio to dip below the Standard Model prediction. This decay is particularly important since it could be the first unambigious signal of new physics at the LHC and also guide the future LHCb upgrade.

Declaration

This dissertation is the result of my own work, except where explicit reference is made to the work of others, and has not been submitted for another qualification to this or any other university. The research described in this thesis was carried out in collaboration with Professor Athanasios Dedes and Professor Janusz Rosiek. Chapters 4 and 5 are based on the work

- A. Dedes, J. Rosiek, P. Tanedo, *Complete One-Loop MSSM Predictions for $B_{s,d} \to \ell^+ \ell'^-$ at the Tevatron and LHC*, IPPP-08-96, `arXiv:0812.4320 [hep-ph]`.

Philip Tanedo
6 May 2008
(Revised 14 January 2009)

Acknowledgements

I would like to express my deep appreciation to my mentor, Professor Athanasios Dedes, for sharing his passion for physics. His guidance and advice, manifested in lunchtime conversations, chalkboards, telephone calls, and e-mails, have helped me grow as a young physicist and have pointed me in the right direction on my research career. I would also like to thank our collaborator, Professor Janusz Rosiek, for his encouragement and suggestions as I developed my program for calculating the $B_{s,d} \to \ell^+ \ell'^-$ branching ratio. The time I've spent comparing and scrutinising our codes have given me a deeper understanding of the structure of the MSSM and the techniques used in computational HEP phenomenology.

Next I would like to express my gratitude to Professors Nigel Glover and Mike Pennington of the Institute for Particle Physics Phenomenology at the University of Durham for accommodating me as a Research MSc student. The IPPP is a very special place in the UK particle physics community and I've been very fortunate to have had the chance to spend the past year there. During this time I've learned a lot from my fellow students. In particular, I'd like to thank my friends and officemates: Dave Wilson for lending his Linux expertise, Aoife Bharucha for many discussions about B physics, Eimear O'Callaghan for lending me her books, Jaime Tattersall and Alison Fowler for discussions about supersymmetry, Josie Huddleston for unexpected jokes, Javier Cobos-Martinez for stoic North American camraderie, and Tracey Li for discussions about neutrino physics. Also, my physicist-flatmates Jonathan Powell, Jo Benjamin, and Ares Perides helped fill my domestic life with interesting discussions about science. I'd like to thank the lecturers of Durham's Centre for Particle Theory taught MSc course for allowing me to sit in on their excellent classes.

I would like to thank the Division of Theoretical Physics at the University of Ioannina, in particular Professors Athansios Dedes and Panagiota Kanti, for their very kind hospitality during part of this work. I am also very grateful to the IPPP for making it possible for me to visit the University of Ioannina.

Parts of this work were presented at the 2007 UK LHCb workshop (Durham, UK), Theory Division Journal Club (Ioannina, GR), CPT Student Seminars (Durham, UK), the 2008 Institute of Physics Annual High Energy Particle Physics meeting (Lancaster, UK), the 5th Annual Part III Return Conference (Cambridge, UK), and the 2008 Marshall Aid Commemoration Commission colloquium for graduating Marshall Scholars (London, UK). I would like to thank the organisers of these events for their generosity in having me and the fantastic discussions generated.

I am supported by a 2006 Marshall Scholarship administered by the Marshall Aid Commemoration Commission. I would like to thank the British Counsulate-General of Los Angeles and the Marshall Commission for making this work possible. Special thanks go to MACC administrators Mary Denyer, Elizabeth Martin, and Natasha Bevan for looking out for the Marshall Scholars; if not for them I would certainly still be lost in Heathrow airport.

In this sense this thesis is the result of two years of study in the United Kingdom. I would like to thank the many other people who have made this journey very special. At Cambridge I'm especially indebted to Suchitra Sebastian for continuing to be a non sequitur role model, Steffen Gielen for camraderie through many memorable Part III adventures, and Evan Keane for getting me out of my books to play basketball regularly. Part III's greatest assets are its students, and my experience owes a lot to Matt Dolan, Olga Goulko, James Holloway, Sven Krippendorf, Hwasung 'Mars' Lee, David Simmons-Duffin, and Leo Van Nierop. I am indebted to Dr. Benjamin Allanach, Dr. David Tong, and Professor Fernando Quevedo for their mentorship and guidance. At Durham, in addition to those thanked above, I'd like to express my graditude to Bader Obeidat, Liz Ellis, Hayley German, Georg Blaser, Lucina Donnachie, Zubi Al-Zubi, Liz New, and Li Geng for their friendship and summer adventures. And among my fellow expatriate scholars, I'd like to thank in particular Adam Morgan, Gregory Sutton, and Allison Bishop for their camaraderie as strangers in a strange land.

This humble work is dedicated to the *fratelli fisici* of the physics blogosphere. It is also dedicated to the memory of Professors Sidney Coleman (1937-2007) and John Archibald Wheeler (1911-2008), two of the great physicists of the 20th century who have sadly passed away over the last year.

Preface

This thesis describes my research in the rare decay processes $B_{s,d} \to \ell^+ \ell'^-$. In particular, I will focus on the phenomenologically interesting process $B_s^0 \to \mu^+ \mu^-$ in the Minimal Supersymmetric Standard Model at low $\tan\beta$ and possible implications at the LHCb experiment. While the results derived herein are complete and independent, this work is a part of a larger project to study the full, one-loop structure and parameter space for $B_{s,d} \to \ell^+ \ell'^-$ in the MSSM [1].

In Chapters 1 and 2 we provide pedagogical introductions to flavour physics in the Standard Model and the Minimal Supersymmetric Standard Model (MSSM). These chapters provide the background necessary for a reader familiar with quantum field theory and the Standard Model, though not necessarily having any formal background in supersymmetry.

In Chapter 3 we review past work on $B_{s,d} \to \ell^+ \ell'^-$ (and related K decays), highlighting relevant results leading up to the recent interest in this decay mode in the MSSM. The large $\tan\beta$ region of the MSSM has been of general interest due to significant enhancements of the MSSM branching ratio over the Standard Model prediction, making this a fertile decay mode to search for signals of new physics. In this thesis, on the other hand, the primary interest is the small $\tan\beta$ region where the branching ratio for $B_s^0 \to \mu^+ \mu^-$ may dip below the Standard Model prediction. This could lead to a non-discovery of this branching ratio at the LHCb, requiring us to carefully consider the remaining parameter space to optimise the discovery potential of an LHCb upgrade.

The heart of the calculation is described in Chapter 4. We provide a brief introduction to Wilsonian effective field theory and its application to the $B_{s,d} \to \ell^+ \ell'^-$ decay mode. The end result is the branching ratio in terms of known parameters and Wilson coefficients which are functions of the MSSM input parameters. This result is automated into a program which is then set to do a scan over parameter space. The results of this parameter scan in the low $\tan\beta$ region are provided in Chapter 5. We will find a suggestive cancellation region in the $B_s^0 \to \mu^+ \mu^-$ channel that could point to 'life beyond

minimal flavour violation.' We close with a brief discussion of the significance of this channel in the context of our broader study.

To maximise the usefulness of this work, we have collected several results and references in the appendices. Appendix A contains a summary of the notation and conventions used throughout this work. Appendix B reviews the definition of mixing matrices and physical states in association with the diagonalisation of the MSSM mass matrices. Appendix C collects the relevant Fierz identities used to perform the calculations in this work. Appendix D provides a quick guide to deriving simple loop integrals and then lists the relevant analytic forms of the loop integrals for this work. Finally, Appendix E summarises the bulk of the calculations of this work by listing the contributions of each one-loop MSSM diagram to the Wilson coefficients in the expression for the branching ratio.

Contents

1 A Quick Review of Selected Topics in Flavour Physics **2**

1.1 The unbroken electroweak theory 2

1.2 Electroweak symmetry breaking 4

1.3 The CKM matrix as an avatar of flavour physics 6

1.4 FCNCs and the GIM mechanism 8

1.5 Putting it all together 10

2 The MSSM in a Nutshell **12**

2.1 Supersymmetry in words 12

2.2 MSSM field content 14

2.3 MSSM field content in slightly more detail 16

2.4 Interactions in the limit of unbroken SUSY 17

2.5 SUSY and electroweak breaking 20

2.6 The SUSY flavour problem 23

3 A Brief History of $B_{s,d} \to \ell^+ \ell'^-$ **25**

3.1 Looking for new physics: The birds and the Bs 25

3.1.1 The birds: penguin diagrams 26

3.1.2 The 'bees': B mesons 27

3.1.3 $B_{s,d} \to \ell^+ \ell'^-$: Searching for the birds in the Bs 27

3.2 $B_{s,d} \to \ell^+ \ell'^-$ in the Standard Model 30

3.3 $B_{s,d} \to \ell^+ \ell'^-$ in a 2HDM 30

3.4 $B_{s,d} \to \ell^+ \ell'^-$ in the MSSM with large $\tan\beta$ 31

3.5 $B_{s,d} \to \ell^+ \ell'^-$ in the MSSM with small $\tan\beta$ 35

4 Calculating $B_{s,d} \to \ell^+ \ell'^-$ **37**

4.1 Effective field theory overview 37

4.2 Effective Operators 39

4.3 Simplification by factorisation 41
4.4 Branching Ratio 43
4.5 QCD corrections 44
4.6 Diagrams and matching 46
4.7 Computational approach 48

5 Physics Results and Conclusions **49**
5.1 General analysis 49
5.2 Scan of parameter space 50
5.3 Outlook 54

A Notation and Conventions **56**

B Diagonalisation of MSSM masses **58**
B.1 Electroweak symmetry breaking 58
B.2 Gauge bosons 59
B.3 Charged scalar Higgses 59
B.4 Neutral scalar Higgses 60
B.5 Standard Model fermions 61
B.6 Charginos 61
B.7 Neutralinos 61
B.8 Gluinos 62
B.9 Sneutrinos 62
B.10 Selectrons 63
B.11 Up squarks 63
B.12 Down squarks 64

C Fierz Identities **65**
C.1 Fierz identities without a C-matrix 66
C.2 Fierz identities with a C-matrix 66

D Loop Integrals **67**
D.1 Algebraic techniques for simple loop integrals 68
D.2 Useful loop integral results 70

E Wilson coefficients **72**
E.1 Feynman Rules 72
E.1.1 Box Diagram Contribution 73

E.1.2 Z-penguins 76
E.1.3 d self-energy contributions 78

Bibliography **82**

List of Figures **85**

List of Tables **87**

"How to calculate
B to mu-plus mu-minus?
This is what I did."
— A haiku

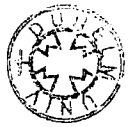

Chapter 1

A Quick Review of Selected Topics in Flavour Physics

> *"It'd be funny if flavour were the only place where new physics showed up at the LHC. Such a next-to-nightmare scenario is not so unlikely."*
> — Jester, *Resonaances* [2]

We begin by reviewing key features of the Standard Model flavour sector. We shall highlight the origin of the Standard Model's flavour structure to form a foundational understanding of the richer flavour structure of the Minimal Supersymmetric Standard Model in the next chapter. Detailed reviews on the Standard Model and flavour physics can be found in the text by Cheng and Li [3] or the more recent text by Burgess and Moore [4].

1.1 The unbroken electroweak theory

The Standard Model is obtained by spontaneously breaking an $SU(3)_C \times SU(2)_L \times U(1)_Y$ nonabelian gauge theory into a $SU(3)_C \times U(1)_{EM}$ theory via the Higgs mechanism. The field content and its representations under the unbroken gauge group is listed in Table 1.1.

Field	Spin	$SU(3)_C$	$SU(2)_L$	$U(1)_Y$
Q	$\frac{1}{2}$	$\mathbf{3}$	$\mathbf{2}$	$\frac{1}{6}$
u^c	$\frac{1}{2}$	$\overline{\mathbf{3}}$	$\mathbf{1}$	$\frac{2}{3}$
d^c	$\frac{1}{2}$	$\overline{\mathbf{3}}$	$\mathbf{1}$	$-\frac{1}{3}$
ℓ	$\frac{1}{2}$	$\mathbf{1}$	$\mathbf{2}$	$-\frac{1}{2}$
e^c	$\frac{1}{2}$	$\mathbf{1}$	$\mathbf{1}$	-1
ϕ	0	$\mathbf{1}$	$\overline{\mathbf{2}}$	$\frac{1}{2}$
g	1	$\mathbf{8}$	$\mathbf{1}$	0
A	1	$\mathbf{1}$	$\mathbf{3}$	0
B	1	$\mathbf{1}$	$\mathbf{1}$	0

Table 1.1: Standard Model particle spectrum and quantum numbers.

The superscript c refers to charge conjugation, $\psi^c = i\gamma^2\psi^*$ in the Dirac representation. All fermions above are left-chiral so that, e.g., u is a *right*-chiral field. We have normalized the hypercharge generator Y such that the electromagnetic charge is $Q_{EM} = T_3 + Y$, where T_3 is the third $SU(2)_L$ generator. We have suppressed an all-important flavour index $i = 1, 2, 3$ on each fermion species. Finally, the $SU(2)_L$ doublets have components

$$Q = \begin{pmatrix} u \\ d \end{pmatrix} \qquad \ell = \begin{pmatrix} e \\ \nu \end{pmatrix}.$$

When necessary, we will explicitly write the chirality to distinguish between the fields coming from the $SU(2)_L$ doublets Q and ℓ from the $SU(2)_L$ singlets u, d, e and ν. For example, we will write u_L to refer to the left-chiral field coming from the first component of Q and u_R to refer to the right-chiral singlet. For the purpose of this work we shall take the strict pre-1998 Standard Model particle content with no right-handed neutrino. The corrections to the $B_{s,d} \to \ell^+ \ell'^-$ calculation, we shall see, are suppressed by a factor $\mathcal{O}(m_\nu/M_W)$.

The Lagrangian before electroweak symmetry breaking is the most general renormalisable Lagrangian that obeys the $SU(3)_C \times SU(2)_L \times U(1)_Y$ gauge symmetry as well as a chiral symmetry that prohibits fermion mass terms. It takes the form

$$\mathcal{L} = \mathcal{L}_{\text{Kin.}} - V_\phi - V_{\text{Yuk.}}, \tag{1.1}$$

where the massless kinetic terms, Higgs potential, and Yukawa potential are respectively

$$\mathcal{L}_{\text{Kin.}} = \overline{\psi}_F i \not{D} \psi_F + |D_\mu \phi|^2 - \frac{1}{4} F^a_{\mu\nu} F^{a\mu\nu} \tag{1.2}$$

$$+V_\phi = -\mu^2 \phi^\dagger \phi + \lambda \left(\phi^\dagger \phi\right)^2 \tag{1.3}$$

$$-V_{\text{Yuk.}} = \tilde{\phi} \cdot \overline{Q} \mathbf{y_u} u_R + \phi \cdot \overline{Q} \mathbf{y_d} d_R + \phi \cdot \overline{\ell}_L \mathbf{y_e} e_R + \text{h.c.}. \tag{1.4}$$

In the above equations we have written F to label all fermions in Table 1.1, a to label the generators of the complete unbroken gauge group, $\tilde{\phi}$ to represent the $SU(2)_L$ conjugate of the Higgs field $\tilde{\phi} = i\tau_2 \phi^*$, the dot $(\cdot)$ to represent contraction of $SU(2)_L$ indices, and $\mathbf{y_F}$ to be the flavour space matrix of Yukawa couplings for the various fermions.

The terms in $\mathcal{L}_{\text{Kin.}}$ and V_ϕ respect a global flavour symmetry

$$SU(3)^5 = SU(3)^Q \times SU(3)^u \times SU(3)^d \times SU(3)^\ell \times SU(3)^e$$

defined by rotating each field in flavour space. However, the Yukawa potential, $V_{\text{Yuk.}}$, does not respect this flavour symmetry since it mixes left- and right-chiral fields from different generations. That is to say that the Yukawa matrices $\mathbf{y_F}$ are not diagonal.

1.2 Electroweak symmetry breaking

Upon electroweak symmetry breaking, the Higgs field ϕ settles to the minumum of its potential. We can choose coordinates such that its vacuum expectation value (vev) is

$$\langle \phi \rangle = \frac{1}{\sqrt{2}} \begin{pmatrix} 0 \\ v \end{pmatrix},$$

where $v = (\mu^2/\lambda)^{\frac{1}{2}}$. Making this replacement in the Yukawa terms turns equation (1.4) into a set of mass terms for the quarks and charged leptons,

$$-V_{\text{Yuk.}} \xrightarrow{EWSB} \mathcal{L}_{\text{mass}} = \overline{u}_L \mathbf{m_u} u_R + \overline{d}_L \mathbf{m_d} d_R + \overline{e}_L \mathbf{m_e} e_R + \text{h.c.}, \tag{1.5}$$

where we've defined the mass matrices $\mathbf{m_F} = \frac{v}{\sqrt{2}} \mathbf{y_F}$. Note that these matrices carry the same flavour structure as the Yukawa matrices and are *not* diagonal.

The propagating states of a theory are eigenstates of the Hamiltonian. Hence the chiral fermions written in Table 1.1 are not physically propagating states. In order to find these states, we must diagonalise the mass (i.e. the Yukawa) matrices. These matrices are generally diagonalised through a biunitary transformation, $\hat{\mathbf{M}} = \mathbf{S}^\dagger \mathbf{M} \mathbf{T}$, where we've designated the diagonal matrix with a hat. Thus we can write:

$$\mathcal{L}_{\text{mass}} = \overline{u}_L \mathbf{S_u} \hat{\mathbf{m}}_\mathbf{u} \mathbf{T}_\mathbf{u}^\dagger u_R + \overline{d}_L \mathbf{S_d} \hat{\mathbf{m}}_\mathbf{d} \mathbf{T}_\mathbf{d}^\dagger d_R + \overline{e}_L \mathbf{S_e} \hat{\mathbf{m}}_\mathbf{e} \mathbf{T}_\mathbf{e}^\dagger e_R + \text{h.c.}, \tag{1.6}$$

The $SU(3)^5$ flavour symmetry of the rest of the Lagrangian gives us the freedom to rotate our fields in flavour space to attempt to diagonalise the above masses. One would like to absorb the unitary matrices $\mathbf{S}$ and $\mathbf{U}$ into the definitions of the chiral fermions. We are unable to do this completely, however, since the u_L and d_L fields are part of the $SU(2)_L$ doublet field Q, and they must rotate the same way in flavour space and hence cannot absorb both the $\mathbf{S_u}$ and $\mathbf{S_d}$ rotations.

By convention we diagonalise the up-quark sector. Focusing on the quarks, let us redefine the fields:

$$Q_L \rightarrow Q'_L = \mathbf{S_u} Q_L \tag{1.7}$$

$$u_R \rightarrow u'_R = \mathbf{T_u} u_R \tag{1.8}$$

$$d_R \rightarrow d'_R = \mathbf{T_d} d_R. \tag{1.9}$$

We then are able to write the mass terms for the quark sector as

$$\mathcal{L}_{\text{mass}} = \overline{u}'_L \hat{\mathbf{m}}_\mathbf{u} u'_R + \overline{d}'_L \underbrace{\mathbf{S}_\mathbf{u}^\dagger \mathbf{S_d}}_{\mathbf{V_{CKM}}} \hat{\mathbf{m}}_\mathbf{d} d'_R + \text{h.c.}. \tag{1.10}$$

We define the **Cabbibo-Kobayashi-Maskawa** (CKM) **matrix** $\mathbf{V_{CKM}} = \mathbf{S}_\mathbf{u}^\dagger \mathbf{S_d}$ to be the unitary flavour mixing matrix in the down quark sector 'leftover' from completely diagonalising the up quark sector. The physical mass eigenstates that propagate are rotated with respect to the flavour (interaction) eigenstates by angles encoded in the CKM matrix.

Have the flavour space rotations of our fermions changed any other part of our Lagrangian? Recall that the covariant derivative takes the form

$$D_\mu = \partial_\mu - i\frac{g}{2}\tau \cdot A_\mu - i\frac{g'}{2}B_\mu. \tag{1.11}$$

In particular, the A_1 and A_2 terms contain the off-diagonal Pauli matrices τ_1 and τ_2 which, in the quark kinetic terms, mix the left-handed up quarks with the right-handed down quarks and vice-versa. Upon electroweak symmetry breaking, the linear combination of A fields that mediates this interaction is identified with the $W^\pm$ boson. The flavour space rotations we made then diagonalising the quark mass matrices then introduce factors of $\mathbf{S_u^\dagger S_d}$ and its hermitian conjugate, i.e. they precisely introduce factors of the CKM matrix. Thus the charged weak current mediates tree-level flavour transitions between up- and down-type quarks with a mixing determined by the CKM matrix.

Unless otherwise specified, we will work in the mass eigenbasis for the remainder of this thesis and will thus drop the primes and hats decorating the fields and matrices above. Further, unless there is an ambiguity, we shall drop the subscript 'CKM' and refer to the CKM matrix as $\mathbf{V}$.

1.3 The CKM matrix as an avatar of flavour physics

The CKM matrix is the heart of heavy flavour physics[1]. In this subsection we take a brief detour to mention two salient features of the CKM matrix that provide a broader context for why physicists are interested in flavour strucutre.

First we note that a large part of the current experimental flavour physics programme is dedicated to accurate measurements of 'unitarity triangles.' These are formed by noting that for a unitary matrix such as the CKM matrix, $\mathbf{V^\dagger V} = \mathbb{1}$. Hence one can consider off-diagonal elements of this product, such as the *bd* (3-1) element:

$$\begin{aligned} 0 &= \left(V^\dagger V\right)_{bd} && (1.12)\\ &= V_{ub}^* V_{ud} + V_{cb}^* V_{cd} + V_{tb}^* V_{td} && (1.13)\\ &= 1 + \left(\frac{V_{cb}^* V_{cd}}{V_{ub}^* V_{ud}}\right) + \left(\frac{V_{tb}^* V_{td}}{V_{ub}^* V_{ud}}\right). && (1.14) \end{aligned}$$

Each term in the final line is a complex number that can be represented as a vector on the complex plane. The fact that these numbers sum to zero mean that the vectors can be arranged into a triangle. This is demonstrated in Figure 1.1. These angles can be

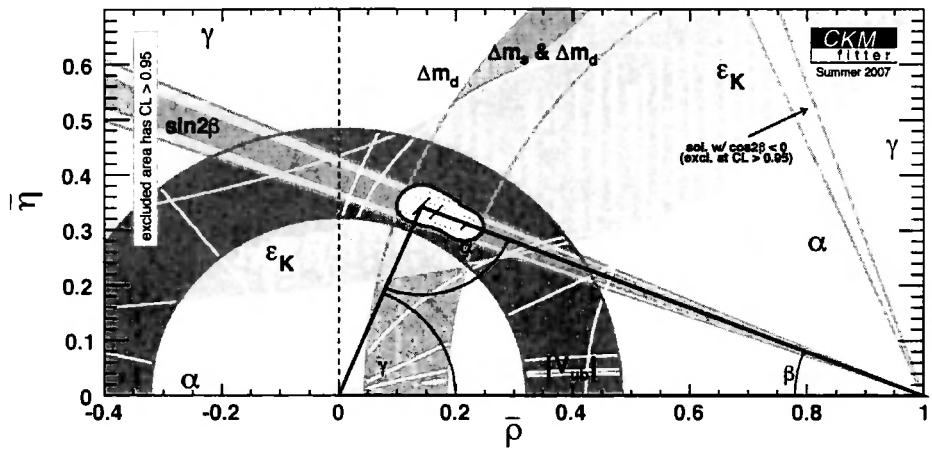

Figure 1.1: Example of a unitarity triangle [5].

measured experimentally by looking at flavour-changing decays which are proportional to elements of $\mathbf{V}^\dagger\mathbf{V}$.

The second feature to note is that the physics of flavour is the physics of CP-violation. In other words, flavour physics probes questions about why we observe a matter-antimatter asymmetry in our universe. This can be seen by a quick analysis of the CKM matrix. Consider the Standard Model with N flavours. Then the CKM matrix has, by unitarity, N^2 real degrees of freedom. These can be expressed as a set of mixing angles and complex phases. The mixing angles are the parameters one would find if you restricted V to be an orthogonal (i.e. real) matrix. Subtracting the degrees of freedom of an orthogonal $N \times N$ matrix, one finds that the CKM matrix has

$$N^2 - \frac{1}{2}N(N-1) = \frac{1}{2}N(N+1)$$

complex phases. These phases aren't all physical since we have the freedom to rephase each of the $2N$ chiral quark fields. As a final subtlety, the overall phase of *all* quarks is a symmetry of the action and hence we can only absorb $2N-1$ of these complex phases. Thus the total number of *physical* complex phases in the N-flavour CKM matrix is

$$\frac{1}{2}N(N+1) - (2N-1) \;=\; \frac{1}{2}(N-1)(N-2). \tag{1.15}$$

[1]The adjective 'heavy' is meant to distinguish this from leptonic flavour physics relating to neutrino mixing.

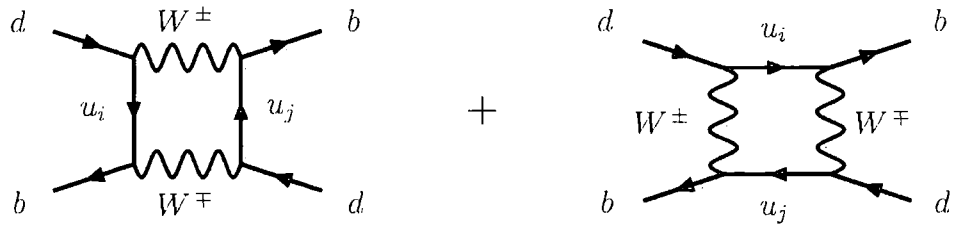

Figure 1.2: Standard Model contribution to $B - \overline{B}$ mixing.

We note, in particular, that for $N = 3$ there is a single complex phase. This phase is responsible for $\mathcal{CP}$ violation in the quark sector. To see this, consider the flavour-changing charged current terms in the Standard Model Lagrangian and its $\mathcal{CP}$ conjugate:

$$\mathcal{L} \supset W_\mu^+ \overline{u_i} V_{ij} \gamma^\mu P_L d_j + W_\mu^- \overline{d_i} V_{ij}^\dagger \gamma^\mu P_L u_j \tag{1.16}$$

$$(\mathcal{CP})\mathcal{L}(\mathcal{CP})^* \supset W_\mu^- \overline{d_j} V_{ij} \gamma^\mu P_L u_i + W_\mu^+ \overline{u_j} V_{ij}^\dagger \gamma^\mu P_L d_i. \tag{1.17}$$

Noting that i and j are dummy flavour indices that are summed over, one can see that if the CKM matrix were purely real, then equations (1.16) and (1.17) are equivalent. In other words, it is the imaginary phase in the CKM matrix that causes the Standard Model to break $\mathcal{CP}$ invariance and treat particles differently from antiparticles. It is clear, then, that flavour physics is the study of why antimatter is different from matter.

1.4 FCNCs and the GIM mechanism

We saw above that the charged weak currents mediated tree-level flavour-changing interactions. Following the same steps, one notes that tree level flavour-changing neutral currents (FCNCs) are prohibited because the unitary tranformations between two left-handed up (down) quarks will cancel one another identically. FCNCs, however, are permitted via loop-mediated processes, albeit suppressed by what is called the **Glashow-Iliopoulos-Maiani** (GIM) **mechanism**. This will be important for our analysis of $B_{s,d} \to \ell^+ \ell'^-$ since the hadronic part of this process is a FCNC.

As an illustrative example, consider $B^0 - \overline{B}^0$ mixing in the Standard Model. The diagrams contributing to this process are shown in Figure 1.2. A detailed calculation isn't necessary, to demonstrate the GIM mechanism. Instead, let us estimate the amplitude

for this process. First, by dimensional analysis, we know that the effective operator in the Lagrangian mediating the $\bar{b}b\bar{d}d$ interaction must have mass dimension -2. Alternately, we can note that the process contains a momentum integral whose mass dimension is -2. The characteristic scale for this integral is given by the mass of the W boson, and hence we begin with a factor of M_W^{-2}. The loop gives us the usual factor of $1/(4\pi)^2$, and each vertex gives a factor of the weak coupling g. In addition, each vertex gives the appropriate factors of the CKM matrix or its hermitian conjugate, which one can see amounts to a factor of $(\sum_i V_{ib}^* V_{id})^2$. A factor of 2 should also be inserted to account for the two diagrams. Thus far we have written

$$\mathcal{O}_{\bar{b}b\bar{d}d} \approx \frac{2g^4}{(4\pi)^2}\frac{1}{M_W^2}\left(\sum_i V_{ib}^* V_{id}\right)^2 . \tag{1.18}$$

This approximates the effective operator. In order to convert it to an approximation for the amplitude, we must insert the appropriate dimensionful kinematic factor to make it dimensionless. Usually this factor is the centre of mass energy, $E_{CM} \approx M_{B^0}$. However, we note that then the entire amplitude would vanish by the unitarity of $\mathbf{V}$:

$$\sum_i V_{ib}^* V_{id} = 0. \tag{1.19}$$

This is, in essence, the same relation we used in showing how unitarity triangles are formed. Hence the only non-vanishing contributions to the $B^0 - \overline{B}^0$ amplitude are terms that introduce a flavour structure that 'disrupts' this matrix multiplication. Fortunately such a structure is available: the up-type quark propagators contain factors of quark masses m_{u_i} in their denominators. Indeed, this factor is necessary enforce that all fermions participating in this weak ($SU(2)_L$) process are left-chiral. The quark masses are 'small' compared to the energy scales of the system, $m_{u_i} \ll M_W, M_{B^0}$ and so we may Taylor expand in them to insert the appropriate factors of m_{u_i} into our amplitude. This argument breaks down for the top quark whose mass is larger than M_W, M_{B^0}. However, the smallness of the V_{td} matrix element ($|V_{td}| \ll 1$) makes the contribution with intermediate tops negligible. Thus we find that the amplitude is approximated by

$$\mathcal{A} \approx \frac{2g^4}{(4\pi)^2}\frac{1}{M_W^2}\left(\sum_i V_{ib}^* V_{id} m_{u_i}\right)^2 . \tag{1.20}$$

One more step must be taken. We note that if the quark masses m_{u_i} were degenerate (i.e. $m_{u_i} = m_u$), then they would factor out of the product of CKM matrices and the

amplitude would again be identically zero. So it is, in fact, the *differences* of the quark masses that lead to non-vanishing amplitudes. With this in mind, instead of Taylor expanding in the quark masses themselves, we can Taylor expand in the differences of the quark masses Δm_{u_i} from an a characteristic reference mass (say m_u), i.e.

$$\frac{1}{\not{p} - m_{u_i}} = \frac{1}{(\not{p} - m_u) - \Delta m_{u_i}} \tag{1.21}$$

$$= \frac{1}{\not{p} - m_u} - \frac{1}{(\not{p} - m_u)^2}\Delta m_{u_i} + \cdots . \tag{1.22}$$

Hence, finally, we can write our expression for the amplitude as

$$\mathcal{A} \approx \frac{2g^4}{(4\pi)^2}\left(\sum_i V_{ib}^* V_{id}\frac{\Delta m_{u_i}}{M_W}\right)^2 . \tag{1.23}$$

The most important feature here is that the amplitude is suppressed both by the smallness of off-diagonal elements of the CKM matrix, but also by the smallness of the quark mass splittings with respect to the W boson mass. This is also the reason why we can neglect the right-handed neutrino in this study. We shall see that the box diagrams contributing to $B_{s,d} \to \ell^+ \ell'^-$ are analogous to the left diagram of Figure 1.2 with the out-states replaced by leptons coupling to a neutrino. By the GIM mechanism, the amplitude is thus suppressed by a factor of $\Delta m_\nu / M_W \ll 1$.

1.5 Putting it all together

We've seen how flavour structure comes out of the Standard Model and how this leads to loop-level flavour-changing neutral currents. These FCNCs are suppressed via loop factors, the smallness of off-diagonal CKM matrix elements, and by the GIM mechanism. We shall see in the following chapter how the supersymmetric Standard Model introduces analogous flavour structure into the theory with additional particle content and couplings. The important feature is that these new particles can influence Standard Model processes by contributing to loop corrections. For decays which occur only at loop-level, such as $B_{s,d} \to \ell^+ \ell'^-$, the contribution from new physics can significantly alter the branching ratio from the Standard Model prediction. This would then be a 'smoking gun' signature for physics beyond the Standard Model.

It is important to note that a measurement of this decay mode alone does not constrain the particular type of new physics. However, in concert with data from high-energy experiments (ATLAS, CMS, ILC) and other low-energy observables (other B decay modes, astro/cosmo-particle experiments) one can begin to piece together the particle spectrum and flavour structure of what lies beyond the Standard Model. We focus here on a particular scenario of new physics, supersymmetry, as a case study for what sorts of discrepancies from the Standard Model one could expect in the $B_{s,d} \to \ell^+ \ell'^-$ channel. We shall see in Chapter 3 that supersymmetry can produce particularly robust signals in this sector.

Chapter 2

The MSSM in a Nutshell

> *"So in supersymmetry, you have superfields and superpotentials and everything is 'super.' At some point this naming convention becomes rather ridiculous, doesn't it? Why not 'hyper'? I'll invent my own theory and call it 'hypersymmetry;' then everything will be 'hyper.'"*
>
> — Steffen Gielen, 2007 Mayhew Prize Recipient

In this chapter we briefly review the construction of the Minimal Supersymmetric Standard Model and identify its flavour structure. We focus on the 'standard canon' of SUSY which are readily described in most texts and reviews such as Bailin and Love [6] or Martin [7]. We shall focus only on developing a 'working knowledge' of the model's field content and relevant couplings rather than delving in to the rich structure of supersymmetry. In particular, we shall avoid detailed discussions of the MSSM kinetic terms, off-shell auxilliary fields, superspace, and generalities of SUSY gauge theories. Readers are directed to the above references for further details on these topics.

2.1 Supersymmetry in words

Supersymmetry (SUSY) can be viewed as an extension of spacetime by quantum Grassmanian dimensions, promoting the usual Minkowski space to a superspace. By doing this it extends the usual Poincaré spacetime symmetry group, and hence extends representations of particles living on the space. At the particle-level, this manifests itself

Figure 2.1: Illustration of one-loop corrections to the Higgs mass from (a) fermions and (b) scalars.

as a symmetry relating integer-spin bosons and half-integer-spin fermions such that every boson of spin s has a supersymmetric fermionic partner of spin $s \pm \frac{1}{2}$. In slightly more pedestrian language, supersymmetry is a correspondence between 'force mediating particles' and 'matter particles.'

SUSY has arguably been the favourite candidate for beyond-the-Standard Model physics for the past thirty years. One of its most appealing model-building features is the cancellation of the quadratic divergence in the Higgs mass. For general gauge theories, chiral and gauge symmetries can be invoked to explain why mass terms for the fermions and gauge bosons are naturally much smaller than the theory's cutoff Λ. However, scalar particles such as the Higgs have no such protection. The scalar squared mass develops a quadratic divergence from the diagrams in Figure 2.1. Thus one would expect the Higgs mass to be on the order of the Standard Model cutoff scale which, naively, might be very large. The mismatch between such a large Higgs mass and the electroweak symmetry breaking phenomena dependent on it is called the hierarchy problem. In the limit of exact SUSY, however, the divergences from a particle running in one diagram cancel against the divergences from the particle's superpartner in the other diagram. Thus the Higgs mass only runs logarithmically and can be naturally small compared to the cutoff.

Additional generic features of SUSY models are grand unification and dark matter. The particle content of supersymmetric versions of the Standard Model (see below) are such that the $SU(3)_C \times SU(2)_L \times U(1)_Y$ gauge couplings unify at some higher scale consistent with LEP data. Further, in order to suppress proton decay operators, it is conventional to impose a discrete R-parity symmetry. This makes the lightest supersymmetric particles (LSP) stable, hence providing a natural dark matter candidate. Supersymmetry has been of more formal interest as the maximal extension of the Poincaré symmetry

under the constraint of the Coleman-Mandula no-go theorem, and for its applications to solitons/instantons in nonperturbative physics and index theorems in mathematics.

Supersymmetry is a beautiful theoretical construct from a mathematical and phenomenological perspective. However, there is a lesson to be taken from Persian rug-makers who used to introduce imperfections in ther rugs so as not to be an affront to the perfection of God. Nature has apparently deemed SUSY 'too beautiful' and has decided to live in a state of broken supersymmetry, as evidenced by the blatant absence of superpartners of the Standard Model particles. We will see that the way in which SUSY is broken has profound ramifications for a model's flavour structure.

2.2 MSSM field content

It is important to note is that nature has a large range of possible high-scale ($M_{\text{SUSY}} \gg$ TeV) theories incorporating supersymmetry in different ways. Such high-scale theories might include multiple ($\mathcal{N} > 1$) supersymmetries or one of a large number of possible SUSY breaking mechanisms. Near the TeV scale, however, the chiral nature of the Standard Model and cancellation of the chiral anomaly within each *generation* (rather than for each particle) imply that the effective theory can only have $\mathcal{N} = 1$ supersymmetry since higher supersymmetries are inherently non-chiral [6]. Further, our motivation for low-scale SUSY constrains the form of the effective TeV-scale SUSY-breaking operators to the so-called soft-breaking terms. Finally, we constrain our field content to the Standard Model fields and their supersymmetric partners. In this way construct the **Minimal Supersymmetric Standard Model** (MSSM) as the unique minimal model of low-energy supersymmetry. The variety of high-scale models manifests itself in a large MSSM parameter space with $\mathcal{O}(100)$ variables, but the low-energy particle content and the constraint to soft-breaking terms allows us to make meaningful statements about phenomenology.

Let us now begin to put together the pieces required for constructing the MSSM. We begin my promoting the Standard Model field content of Table 1.1 to superfields, which are SUSY multiplets of paired bosonic and fermionic degrees of freedom. One modification is necessary: the fermionic superpartner of the Higgs field, the Higgsino, is a new fermion with nontrivial $SU(2)_L$ quantum number. In order to maintain the cancellation of the chiral anomaly which occured within each generation of the Standard Model, we must include a second Higgs superfield to the theory. Thus the MSSM

Superfield	Boson	Fermion	$SU(3)_C$	$SU(2)_L$	$U(1)_Y$
Q	Scalar	Weyl	$\mathbf{3}$	$\mathbf{2}$	$\frac{1}{6}$
U^c	Scalar	Weyl	$\overline{\mathbf{3}}$	$\mathbf{1}$	$\frac{2}{3}$
D^c	Scalar	Weyl	$\overline{\mathbf{3}}$	$\mathbf{1}$	$-\frac{1}{3}$
ℓ	Scalar	Weyl	$\mathbf{1}$	$\mathbf{2}$	$-\frac{1}{2}$
E^c	Scalar	Weyl	$\mathbf{1}$	$\mathbf{1}$	-1
H_u	Scalar	Weyl	$\mathbf{1}$	$\overline{\mathbf{2}}$	$\frac{1}{2}$
H_d	Scalar	Weyl	$\mathbf{1}$	$\mathbf{2}$	$-\frac{1}{2}$
g	Vector	Majorana	$\mathbf{8}$	$\mathbf{1}$	0
A	Vector	Majorana	$\mathbf{1}$	$\mathbf{3}$	0
B	Vector	Majorana	$\mathbf{1}$	$\mathbf{1}$	0

Table 2.1: MSSM superfield spectrum and quantum numbers.

particle spectrum is that of a Type II two Higgs doublet model (2HDM) with one Higgs coupling to the up-type quarks and the other couplings to the down-type quarks and leptons[1]. Upon electroweak symmetry breaking, each Higgs doublet will acquire a vacuum expectation value. The ratio of these two vevs is the parameter $\tan\beta = \frac{v_u}{v_d}$.

The superfield content of the MSSM before supersymmetry and electroweak symmetry breaking is listed in Table 2.1. We have explicitly written out the types of paired bosonic and fermionic degrees of freedom. The Standard Model 'matter' particles and Higgs fields are contained in chiral multiplets which pair chiral Weyl fermions with complex scalar fields. The Standard Model 'force mediating' particles are contained in vector multiplets which pair Majorana fermions with real vector fields.

A bit of nomenclature is now necessary. We shall identify the fermionic partners of Standard Model bosons by appending the suffix '-ino' to the Standard Model particle name. We shall identify bosonic partners of Standard Model fermions by appending the prefix 's-' to the Standard Model particle name. The Standard Model component of a superfield is denoted by its usual symbol while the supersymmetric partner is generally denoted by adding a tilde above this symbol.

[1]We choose the more intuitive notation where H_d is the doublet coupling to leptons/down quarks while H_u is the doublet coupling to the up quarks. Another common notation is $H_1 = H_d$, $H_2 = H_u$.

2.3 MSSM field content in slightly more detail

It is instructuve to employ slightly more formal language to describe these fields. A casual reader may omit the remainder of this subsection, though it will help quantify the following subsection on generating the MSSM interaction terms. I shall employ the notation of [6], though details regarding signs conventions will not be relevant. Let us define a superfield $\Phi(x^\mu, \theta^\alpha, \theta^{\dot{\alpha}})$ to be a field that takes values over Minkowski space extended by two-component Grassmann spinor directions θ^α and $\overline{\theta}^{\dot{\alpha}}$. In order to recover our usual component fields, we integrate out these directions in our action to generate a Minkowski space theory of bosons and fermions. This is identical to the dimensional reduction of higher dimensional theories, except that the extra dimensions are fermionic rather than bosonic.

The (super)covariant derivatives over this superspace are defined to be

$$\mathcal{D}_\alpha = \frac{\partial}{\partial\theta^\alpha} + i(\sigma^\mu)_{\alpha\dot{\alpha}}\overline{\theta}^{\dot{\alpha}}\frac{\partial}{\partial x^\mu} \tag{2.1}$$

$$\overline{\mathcal{D}}_{\dot{\alpha}} = -\frac{\partial}{\partial\overline{\theta}^{\dot{\alpha}}} - i\theta^\alpha(\sigma^\mu)_{\alpha\dot{\alpha}}\frac{\partial}{\partial x^\mu}. \tag{2.2}$$

Left-handed **chiral superfields** are irreducible SUSY representations that are defined to satisfy

$$\overline{\mathcal{D}}\Phi(x,\theta,\overline{\theta}) = 0. \tag{2.3}$$

Right-handed anti-chiral superfields are defined similarly with

$$\mathcal{D}\bar{\Phi}(x,\theta,\overline{\theta}) = 0, \tag{2.4}$$

though these will not be as relevant for the MSSM.

Because Grassman variables anticommute, it is possible to expand a general superfield as a finite (i.e. terminating) series in the Grassman variable. This expansion makes the Minkowski space field content manifest. For a chiral superfield, the constraint of equation (2.3) implies that it is possible to expand the chiral superfield Φ_χ as

$$\Phi_\chi(y,\theta) = \phi(y) + \sqrt{2}\theta\psi(y) + \theta\theta F(y). \tag{2.5}$$

Here $y = x + i\theta\sigma^\mu\overline{\theta}$ and we have explicitly identified the degrees of freedom associated with a chiral superfield: a complex scalar ϕ, a left-handed Weyl fermion ψ and a non-propagating auxilliary field F that can be integrated out.

Vector superfields are irreducible SUSY representations that are defiend to satisfy

$$\Phi_V^a = \Phi_V^{a\dagger},$$

where a is a gauge index. For SUSY gauge theories, chiral superfields transform as

$$\Phi_\chi \to \Phi'_\chi \;=\; \exp(-2igt^a\Lambda^a)\Phi_\chi, \tag{2.6}$$

where g is a gauge coupling, t^a is the Hermitian generator of the gauge group, and Λ^a is a chiral superfield 'gauge function.' Vector superfields transform as

$$\exp\Phi_V \to \exp\Phi'_V \;=\; \exp(-2igt^a\Lambda^a)\exp\Phi_V\exp(2igt^a\Lambda^a). \tag{2.7}$$

It is possible to make the field content manifest by going into to the Wess-Zumino gauge, in where we may again write the superfield as a terminating expansion in the Grassmanian directions,

$$\Phi_V(x,\theta,\overline{\theta}) \;=\; \theta\sigma^\mu\overline{\theta}V_\mu(x) + i\theta\theta\overline{\theta}\overline{\lambda}(x) - i\overline{\theta}\overline{\theta}\theta\lambda(x) + \frac{1}{2}\theta\theta\overline{\theta}\overline{\theta}D(x). \tag{2.8}$$

Here we have explicitly identified the real vector V_μ, Majorana fermion (gauginos) λ, and another non-propagating auxilliary field D.

2.4 Interactions in the limit of unbroken SUSY

Following the same procedure as section 1.1 for deriving the Standard Model, we would now like to identify the permissible renormalisable interaction terms compatible with our symmetries: global chiral symmetry, $SU(3)_C \times SU(2)_L \times U(1)_Y$ gauge symmetry, and supersymmetry. The Standard Model has already taught us how to write down terms compatible with the first two symmetries. We must now identify the constraints that supersymmetry imposes and what new terms might arise from having an additional Higgs field. We are especially interested in the relevant flavour structure that might arise.

Let us begin with the chiral superfields. It can be shown that the product of chiral superfields is also a chiral superfield. Further, the auxilliary field (F-term) of a chiral superfield is invariant under a supersymmetry transformation up to a total derivative. Hence these are natural terms to construct supersymmetry-invariant interaction terms in the MSSM Lagrangian. The particular linear combination of chiral superfield products that obey our symmetries is called the **superpotential**, W. The restriction to chiral and not antichiral superfields means that the superpotential must be a holomorphic function of superfields. Renormalisability tells us to consider terms with up to three powers of superfields[2]. Restricting to the F-term of such a superpotential, we get the following contrubition to the Lagrangian:

$$\mathcal{L} \supset -\left|\frac{\partial W(\varphi)}{\partial \Phi^i}\right|^2 - \frac{1}{2}\left(\frac{\partial^2 W(\varphi)}{\partial \Phi^i \partial \Phi^j}\psi_i \psi_j + \text{h.c.}\right). \tag{2.9}$$

This comes from Taylor expanding the superpotential around its scalar component φ, taking the F-term, and replacing the auxilliary fields with physical fields through their (algebraic) equations of motion. The first term on the right hand side is a contribution to the scalar potential, the analogue of equation (1.3). The second term, however, gives us a prescription for writing down Yukawa couplings in our theory:

1. Select any a term in the superpotential
2. Set each chiral superfield field to its scalar component
3. Swap any two of those fields with their fermionic components
4. This term is part of the Lagrangian.

For example, the term $H_u QU$ in the superpotential would generate the usual up quark Yukawa coupling ($h_u u_L u_R$) as well as quark-squark-Higgsino ($u\tilde{u}\tilde{H}_u$) Yukawa couplings. In this way we can read off sets of MSSM interactions (before SUSY breaking) from the superpotential the same way we usually read individual interactions from a Lagrangian.

Before writing down the MSSM superpotential, let us note for completeness that the other parts of the Lagrangian do not introduce interesting flavour structure. It is possible to construct a SUSY gauge field strenth and then a corresponding kinetic term for the vector superfields. This indeed provides kinetic terms for the vector field and Majorana fermion field. There is also a quadratic term for the auxilliary field that, upon replacement using its equation of motion, gives a contribution to the scalar potential.

[2]Since $[W|_F] \leq 4$ and $W = \cdots + \theta\theta W|_F$, we must have $[W] \leq 3$ since the Grassmann coordinates have mass dimension $[\theta] = -\frac{1}{2}$

Next one could consider the gauge-invariant kinetic terms of the chiral superfield, the so-called Kähler potential. These give the usual kinetic terms for the chiral scalars and fermions, with the derivative repalced by the gauge covariant derivative. The additional terms include further contributions to the scalar potential, and flavour-diagonal three-point interactions with the gauginos. A complete discussion of the full Feynman rules for the MSSM is given in [8].

Let us now write down an *a priori* superpotential for the MSSM, including all renormalisable interactions consistent with the requisite symmetries. Suppressing flavour indices and couplings for simplicity, we find

$$\begin{aligned} W &= H_u \cdot H_d + H_u \cdot QU^c + H_d \cdot QD^c + H_d \cdot \ell E^c \\ &\quad + \ell \cdot \ell E^c + LH_u + \ell \cdot QD \\ &\quad + UDD. \end{aligned} \tag{2.10}$$

We can see two immediate problems. The interactions on the second line violate lepton number and the interaction on the third line violates baryon number. Such interactions are experimentally constrained to be negligibly small if at all present, and it seems the size of the associated couplings would diagree with naturalness.

Fortunately, we may impose a discrete symmetry called R-parity to remove these offending terms. The R-parity of a superfield is defined as

$$P_R = (-)^{3(B-L)+2s}. \tag{2.11}$$

With this definition all Standard Model fields and the scalar components of the Higgs supermultiplets are R-parity even while their supersymmetric partners have R-parity odd.

Imposing R-parity on the superpotential and restoring the coupling constants and flavour matrices, the superpotential takes the form

$$W = \mu H_u \cdot H_d + H_u \cdot Q\mathbf{y_u}U^c + H_d \cdot Q\mathbf{y_d}D^c + H_d \cdot \ell\mathbf{y_e}E^c. \tag{2.12}$$

The first term is the generalisation of the Higgs mass term in the MSSM. The remaining terms give precisely the Yukawa structure of the Standard Model. At this point, we have not recovered any new flavour structure in the MSSM. The requirement of R-parity can

be thought of as demanding that the MSSM is minimal not only in particle content, but in couplings.

2.5 SUSY and electroweak breaking

The remaining ingredient for the MSSM is to explicitly break supersymmetry, hence introducing mass splittings between the observed Standard Model and their yet-unobserved superpartners. We shall parameterise the effective low-energy manifestation of a generic high-scale SUSY-breaking mechanism in terms of **soft supersymmetry breaking** terms. These are the phenomenologically-viable terms which explicitly break supersymmetry, but maintain gauge symmetry, R-parity, renormalisability, and do not introduce any divergences. The additional terms in the Lagrangian are:

$$\begin{aligned}
\mathcal{L}_{\text{soft}} \;=\; & -m_{H_u}^2 H_u^* H_u - m_{H_d}^2 H_d^* H_d + \left(m_{12}^2 H_u H_d + \text{h.c.}\right) \\
& -\tilde{Q}^* \mathbf{m}_{\tilde{\mathbf{Q}}}^{\mathbf{2}} \tilde{Q} - \tilde{d}^* \mathbf{m}_{\tilde{\mathbf{d}}}^{\mathbf{2}} \tilde{d} - \tilde{u}^* \mathbf{m}_{\tilde{\mathbf{u}}}^{\mathbf{2}} \tilde{u} - \tilde{\ell}^* \mathbf{m}_{\tilde{\ell}}^{\mathbf{2}} \tilde{\ell} - \tilde{e}^* \mathbf{m}_{\tilde{\mathbf{e}}}^{\mathbf{2}} \tilde{e} \\
& + \frac{1}{2} M_1 \tilde{B}\tilde{B} + \frac{1}{2} M_2 \tilde{A}\tilde{A} + \frac{1}{2} M_3 \tilde{g}\tilde{g} + \text{h.c.} \\
& + H_d \tilde{\ell} \mathbf{a}_{\ell} \tilde{e} + H_d \tilde{Q} \mathbf{a}_{\mathbf{d}} \tilde{d} + H_u \tilde{Q} \mathbf{a}_{\mathbf{u}} \tilde{u} + \text{h.c.} \\
& + H_u^* \tilde{\ell} \mathbf{a}'_{\ell} \tilde{e} + H_u^* \tilde{Q} \mathbf{a}'_{\mathbf{d}} \tilde{d} + H_d^* \tilde{Q} \mathbf{a}'_{\mathbf{u}} \tilde{u}
\end{aligned} \tag{2.13}$$

where gauge indices are contracted appropriately.

These terms take the form of mass and three-point scalar couplings. Recall that the boldfaced terms are flavour-space matrices that are generally not diagonal. These terms introduce new flavour structure in the same way that the off-diagonal mass matrices after electroweak symmetry breaking led to the introduction of the CKM matrix. Note that in the final line contains non-holomorphic three-point Yukawa-type scalar couplings.

With SUSY now broken, we can proceed to break electroweak symmetry[3]. This proceeds as usual with the modification of having an extended particle and coupling content. The physical fields are those that arise from diagonalising the mass matrices of the theory, with the theory's flavour structure encoded in the flavour-space mixing matrices used to diagonalise these masses. We shall now highlight the low-energy spectrum of the MSSM and identify the key mixing parameters. I shall use the conventions of [8].

[3]The scalar potential generated for the Higgs bosons generically takes the usual 'Mexican hat' form.

A more comprehensive discussion of the diagonalisation and associated definitions can be found in Appendix B.

- **Gauge bosons**. This sector behaves just as in the Standard Model. The Higgs mechanism breaks the full gauge group to the $SU(3)_C \times U(1)_{EM}$ subgroup. The A and B bosons combine with components of the Higgs doublets to form massive $W^{\pm}$ and Z bosons.
- **Higgs scalars**. The MSSM's two complex scalar $SU(2)_L$ doublets have a total of eight degrees of freedom. Three are 'eaten' by the Higgs mechanism to give masses to the gauge bosons. The remaning physical spectra include the light Higgs h, heavy Higgs H^0, $\mathcal{CP}$-odd Higgs A^0, and the charged complex Higgs $H^{\pm}$.
- **Standard Model fermions**. The quarks and leptons have masses and mixings coming from the Yukawa sector, as in the Standard Model case.
- **Charginos**. The Majorana fermions associated with the off-diagonal $SU(2)_L$ generators A^1 and A^2 mix with the two charged Weyl fermion Higgsinos to form two charged Dirac fermions called charginos, $\chi_{1,2}$. In more conventional words, these are linear combinations of the superpartners to the $W^{\pm}$ bosons.
- **Neutralinos**. The Majorana fermions associated with the B and the diagonal $SU(2)_L$ generator A^3 mix with the two neutral Weyl fermion Higgsinos to form four neutral Majorana fermions called neutralinos, $\chi^0_{1,2}$. In more conventional words, these are linear combinations of the superpartners to the photon and Z boson.
- **Gluinos**. The Majorana fermions associated with the eight gluons do not mix since $SU(3)_C$ is unbroken.
- **Sneutrinos**. The three complex scalar superpartners to the right-chiral neutrinos mix with a mixing matrix within themselves under a unitary matrix Z_ν.
- **Selectrons**. The complex scalar superpartners to the left- and right-chiral electrons mix within themselves under a unitary matrix Z_L.
- **Up squarks**. The compelx scalar superpartners to the left- and right-chiral up quarks mixing within themselves under a unitary matrix Z_U.
- **Down squarks**. The compelx scalar superpartners to the left- and right-chiral down quarks mixing within themselves under a unitary matrix Z_D.

The MSSM spectrum after electroweak symmetry breaking and diagonalisation in flavour-space is summarised in Table 2.2.

Field	Symbol	Type	EM	Mixing matrix, field superposition	
Photon	γ_μ	Vector	0	θ_W	A^3, B
Z-boson	Z_μ	Vector	0	θ_W	A^3, B, G^0
W-boson	$W_\mu^\pm$	Vector	$\pm$	θ_W	$A^{1,2}$, $G^\pm$
Light Higgs	h	Scalar	0	Z_R	$\mathrm{Re}(H_d^1, H_u^2)$
Heavy Higgs	H	Scalar	0	Z_R	$\mathrm{Re}(H_d^1, H_u^2)$
$\mathcal{CP}$-odd Higgs	A^0	Scalar	0	Z_H	$\mathrm{Im}(H_d^1, H_u^2)$
Charged Higgs	$H^\pm$	Scalar	$\pm$	Z_H	H_d^2, H_u^1
Up quark	u^i	Dirac	$+\frac{2}{3}$	$\mathbf{S_u}$	u_L^i, u_R^i
Down quark	d^i	Dirac	$-\frac{1}{3}$	$\mathbf{S_d}$	d_L^j, d_R^j
Electron	e^i	Dirac	$-$	$\mathbf{S_e}$	e_L^i, e_R^i
Neutrino	ν^i	Dirac	0	$\mathbf{S}_\nu$	ν_L^i
Chargino	$\chi_{1,2}$	Dirac	$\pm$	$Z_\pm$	$\tilde{A}^{1,2}, \tilde{H}_u^1, \tilde{H}_d^2$
Neutralino	$\chi_{1,2,3,4}^0$	Majorana	0	Z_N	$\tilde{B}, \tilde{A}^3, \tilde{H}_u^2, \tilde{H}_d^1$
Gluino	$\tilde{g}^{1,\cdots,8}$	Majorana	0	$\mathbb{1}$	$\tilde{g}^{1,\cdots,8}$
Sneutrino	$\tilde{\nu}^i$	$\mathbb{C}$ Scalar	0	$\mathbf{Z}_\nu$	$\tilde{\nu}_L^i$
Selectron	$\tilde{e}^i$	$\mathbb{C}$ Scalar	$-$	$\mathbf{Z_L}$	$\tilde{e}_L^i, \tilde{e}_R^i$
Up squark	$\tilde{u}^i$	$\mathbb{C}$ Scalar	$+\frac{2}{3}$	$\mathbf{Z_U}$	$\tilde{u}_L^i, \tilde{u}_R^i$
Down squark	$\tilde{d}^i$	$\mathbb{C}$ Scalar	$-\frac{1}{3}$	$\mathbf{Z_D}$	$\tilde{d}_L^i, \tilde{d}_R^i$

Table 2.2: MSSM spectrum after electroweak symmetry breaking.

θ_W is the Weinberg angle, representing the usual mixing of the Standard Model electroweak gauge bosons. The Gs are Higgs Goldstone modes from electroweak symmetry breaking. i, j are flavour indices and bolded matrices contain non-trivial flavour structure. The CKM-matrix $\mathbf{V}_{\mathrm{CKM}}$ is formed as in equation (1.10). Similarly, one can form a super-CKM matrix $\tilde{\mathbf{V}}_{\mathrm{CKM}}$ out of $\mathbf{Z_U}$ and $\mathbf{Z_D}$ [9].

2.6 The SUSY flavour problem

The introduction of the Z matrices as new flavour structure in the theory immediately runs up against experiments. The Yukawa couplings between Standard Model fermions and their scalar superpartners permit loop-level processes where the flavour structure of the sparticles is carried into the Standard Model particles. Flavour changing processes in the Standard Model have been probed to good accuracy by experiments and hence the terms leading to the new mixings Z are constrained. The strictest constraints come lepton flavour violating processes such as $\mu \rightarrow e\gamma$. These severely limit the size of the $\mathbf{m}^2_{\tilde{\mathbf{e}}}$, $\mathbf{a_e}$, and $\mathbf{a'_e}$ soft SUSY breaking terms. Similarly, experimental constraints from studies of the D and B mesons limit the corresponding scalar mass and three-point couplings for the squarks.

It turns out that most 'garden variety' (generically off-diagonal) values of the mass matrices are ruled out experimentally and theorists must be a bit more delicate with the flavour structure. In other words, the off-diagonal elements of the mass matrices are experimentally constrained to take *a priori* unnaturally small values. This is called the SUSY flavour problem [10].

One approach to this problem is to suppress the offending terms completely by fixing the SUSY scale (i.e. the scale of the soft-SUSY breaking terms) to be much larger than the TeV scale, hence decoupling the flavour-structure from the low-energy theory. This, however, runs up against the motivation of naturalness for supersymmetry since it introduces a new hierarchy between the weak scale and the SUSY scale. A second approach postulates that the SUSY-breaking mechanism is flavour-blind such that the scalar masses are all proprtional to the unit matrix in flavour space, prohibiting new contributions to flavour-changing processes. This occurs automatically in gauge-mediated SUSY breaking scenarios, and hence new effects in the flavour sector would strongly constrain this scenario. A final approach to the SUSY flavour problem is alternately called alignment or **minimal flavour violation** (MFV). This states that the

flavour structure introduced by the scalar superpartner masses and three-point couplings is exactly the same as the CKM matrix, i.e. that the squarks and quarks are diagonalised by the same rotations in flavour space. This can be motivated through horizontal-symmetries between generations and has become a popular model-building tool in beyond-the-Standard-Model physics.

With the looming LHCb heralding a new generation of flavour experiments promising even higher sensitivity, there has been a renewed effort to study 'beyond-MFV' models with non-trivial flavour structure [11, 12]. It is hoped that upcoming experiments may find small deviations from the Standard Model expectation of flavour-changing observables that could be accounted for by new physics with non-trivial flavour structure, such as the MSSM.

Chapter 3

A Brief History of $B_{s,d} \to \ell^+ \ell'^-$

"We abbreviate supergravity by writing 'SUGRA.' I don't really use this because it sounds too much like the Spanish word for 'mother-in-law.'"

— Fernando Quevedo

In this chapter we begin by highlighting the features of the decay mode $B_{s,d} \to \ell^+ \ell'^-$ as a model-independent fertile hunting-ground for new physics. We give a brief overview of the 'birds and the Bs:' penguin diagrams and B mesons. Finally, we briefly review the literature on $B_{s,d} \to \ell^+ \ell'^-$ in the Standard Model, Type II two Higgs doublet models (2HDM), and finally the MSSM. We will especially explain the significance of the large $\tan\beta$ limit that has generated interest in recent years along with the importance of the small $\tan\beta$ limit that is the focus of this study. We explain the relevance of this work in the context of past calculations and current experiments.

3.1 Looking for new physics: The birds and the Bs

Compared to other particle collider experiments that focus on directly accessing new energy scales, flavour physics experiments generally probe nature at the mesonic scale. Instead of the rational producing new particles on-shell to study their decays directly, these low-energy searches for beyond the Standard Model physics rely on measuring the off-shell quantum interference of new particles on the decays of mesons, i.e. loop effects.

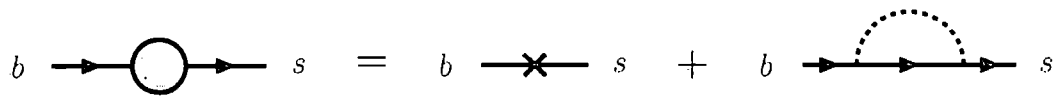

Figure 3.1: Heuristic picture of $b \to s$ transitions and the effect of new physics (dashed line).

We noted in Section 1.5 that flavour-changing neutral currents are a natural place to look for new physics because the loop-level effects of new physics can be pronounced against the Standard Model predictions. We now motivate our interest in the rare decay $B_{s,d} \to \ell^+ \ell'^-$ in this context.

3.1.1 The birds: penguin diagrams

A very heuristic picture of the effect of new physics on a part of a flavour-changing Feynman diagram is portrayed in Figure 3.1. The endpoints of the diagram are understood to be flavour (not mass) eigenstates, the cross is an off-diagonal mass insertion in this flavour-basis. The tree-level process contains no new physics and thus contributes to a large (relative to the loop-suppressed new physics) Standard Model background. At loop-level, we expect that new physics coupling to Standard Model fields will contribute additional diagrams with new particles running in the loops. In this picture, however, the factors of $\mathcal{O}(10)$ mass differences between quark flavours causes decoherence and suppresses the transition[1].

One can relieve the momentum difference between the in- and out-states of Figure 3.1 by allowing the excess momentum to radiate away via, for example, a photon. This photon may then decay into a fermion-antifermion pair. The resulting process is then allowed to occur on-shell and is a robust means for flavour change. This type of diagram is known as a **penguin diagram**[2], and has been suggestively drawn in Figure 3.2.

These penguin processes will play an important role in the upcoming discussion, as they generally do in flavour physics.

[1] In contrast to this, the smallness of the neutrino mass differences permits coherent mixing of neutrino species. For a pedagogical discussion see [13].

[2] The etymology of this term is a well-known page in the history of modern physics. For historical notes, see [14] and [15].

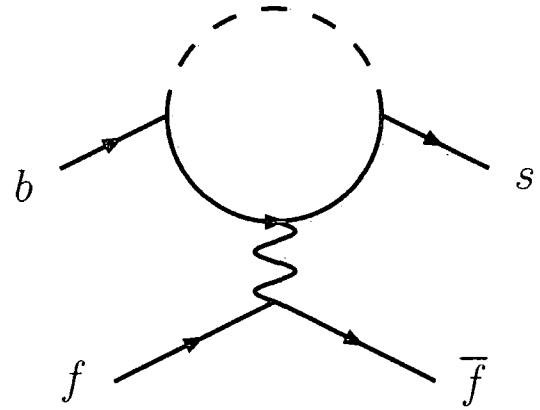

Figure 3.2: A penguin diagram, drawn suggestively to look somewhat avian.

3.1.2 The 'bees': B mesons

The current state-of-the-art laboratory for flavour physics is the B meson. In particular, we shall consider the neutral B_s^0 and B_d^0 mesons, whose basic properties are listed in Table 3.1. The quark content of these mesons are $B_s^0 \equiv \bar{b}s$, $B_d^0 \equiv \bar{b}d$. These particles are especially interesting because they are relatively massive and long-lived, allowing them to be easily tagged in particle detectors. Decays of these mesons probe angles of the CKM matrix that were not directly accessible in the previous generation of K meson experiments.

Meson	Mass	Mean lifetime
B_d^0	5.28 GeV	1.53×10^{-12}s
B_s^0	5.37 GeV	1.44×10^{-12}s

Table 3.1: Properties of the B^0 mesons.

3.1.3 $B_{s,d} \to \ell^+ \ell'^-$: Searching for the birds in the Bs

The search for new physics in the flavour sector, then, can be summarised as the search for the effect on observables of quantum interference from loop-level (e.g. penguin) diagrams. The leading question then is which observables are particularly rich for signals

of new physics. In other words, given that we're looking for penguins, where do we look for them?

If we were to ask biologists this question, the knee-jerk answer we would receive is to look in Antarctica. Why? They would tell us that Antarctica is ideal because (1) *there is very little background*, and (2) *the penguin is the dominant fauna*. This is a trivial statement for anyone who has seen the popular documentary *March of the Penguins* [16]. Silliness aside, we now pose the same question to a flavour phenomenologist. One very good answer to this question is the set of rare decay modes $B_{s,d} \to \ell^+ \ell'^-$. In particular, the mode $B_s^0 \to \mu^+ \mu^-$. The reasons are exactly the same as those for the Antarctic penguins: (1) *there is very little background*, and (2) *the penguin is the dominant diagram*. Let us quatify why this is an especially nice and important mode for searching for new physics.

First of all, the background for a signal of new physics is suppressed. When searching for new physics, one's 'background' are the Standard Model events which contribute to the same process[3]. There are three sources of suppression for the Standard Model process:

- **Loop suppression.** Since the hadronic part of this decay is a FCNC, there are no tree-level diagrams and the first Standard Model contribution comes at one-loop level. Hence diagrams with new particles aren't suppressed by a relative factor of $1/(4\pi)^2$ to a large tree-level background.
- **GIM suppression.** As explained above in section 1.4, the Standard Model decay is also suppressed by a powers of $V_{ib}^* V_{id} \, (\Delta m_{u_i}/M_W)$ via the GIM mechanism. This would mean models of new physics with new flavour structure or a different spectrum of particles in the loop would have the opportunity to stand out.
- **Mass-insertion suppression.** The B^0 particles are spin-0. Hence, by momentum conservation, both the lepton and anti-lepton must have the same helicity (as they travel in opposite directions). Since these flavour-changing decays are mediated by the weak currents, they couple only to left-chiral fermions. Thus the leptonic amplitude must include a mass insertion to swap the helicity of one of the outgoing particles. The process is thus further suppressed by the smallness of the lepton mass to the characteristic scale of the decay.

[3]The term 'background' here is used from a theorist's perspective. An experimentalist would define the background to be those processes which fool the detector that its recording a different process. For example, the main source of experimental background for $B_s^0 \to \mu^+ \mu^-$ is the decay $B_s^0 \to \pi^+ \pi^-$.

Secondly, the experimental signature is very clean. As it is purely leptonic, there are no hadronic effects (e.g. jets) that require careful analysis. Further, since the decay is to two charged leptons, it is a trivial event to tag in the detector. Next, the hadronic uncertainties are restricted to the B^0 meson decay constants (see below). The branching ratio proportional the square of the decay constant, and so this dependence is easily quantified and updated with updated lattice QCD calculations. Finally, and perhaps most importantly, the Standard Model expectation for branching ratio for this process will be experimentally accessible at the upcoming LHCb experiment. The first definite signal for new physics in the LHC could very well come from this decay mode.

In summary, the motivation for looking at $B_{s,d} \to \ell^+ \ell'^-$ is that it is easy to study and has significant discovery potential. The current experimental bounds and Standard Model predictions are listed in Table 3.2. The error in the SM predictions for the $B_{s,d}$

Channel	Expt.	Bound (90% CL)	SM Prediction
$B_s^0 \to \mu^+\mu^-$	CDF II [17]	$< 4.7 \times 10^{-8}$	$(4.7 \pm 1.8) \times 10^{-9}$
$B_d^0 \to \mu^+\mu^-$	CDF II [17]	$< 1.5 \times 10^{-8}$	$(1.8 \pm 0.9) \times 10^{-10}$
$B_s^0 \to \mu^+e^-$	CDF [18]	$< 6.1 \times 10^{-6}$	≈ 0
$B_d^0 \to \mu^+e^-$	BABAR [19]	$< 9.2 \times 10^{-8}$	≈ 0

Table 3.2: Current experimental bounds and SM expectations for leptonic B decays.

branching ratios originates primarily from the uncertainty in the decay constants [20],

$$f_{B_s} = 230 \pm 30 \text{ MeV}$$

$$f_{B_d} = 200 \pm 30 \text{ MeV}$$

linearly added to the top-strange and top-down elements of the CKM matrix, $|V_{ts}| = 0.0406 \pm 0.0027$ and $|V_{td}| = 0.0074 \pm 0.0008$ [21]. The $B_{s,d} \to \tau^+\tau^-$ decay are omitted because current experiments are unable to effectively measure this decay rate.

The lepton flavour violating (LFV) processes would be a clear signal for new physics, though such effects would be very small and are unlikely to be accessibe at current experiments. We shall focus on the phenomenologically interesting and timely $B_s^0 \to \mu^+\mu^-$ mode and later make a note on prospects for the $B_d^0 \to \mu^+\mu^-$ mode.

3.2 $B_{s,d} \to \ell^+ \ell'^-$ in the Standard Model

Inami and Lim were the first to calculate FCNC meson decay into muons with their study of the effect of new particles on K mesons [22]. Their paper includes a full calculation of the relevant Standard Model box and penguin diagrams and analytic formulae for the associated loop integrals. The result for B mesons is obtained by trivially replacing the parameters for the K_L^0 quarks with the appropriate B quark content. The $\mathcal{O}(\alpha_s)$ QCD corrections to the K_L^0 decay were calculated by Buras and Buchalla [23], who found for the $B_s^0 \to \mu^+ \mu^-$ decay:

$$\mathrm{Br}\left(B_s^0 \to \mu^+ \mu^-\right) = 3.5 \times 10^{-9} \left[\frac{\tau_{B_s}}{1.6 \text{ ps}}\right] \left[\frac{f_{B_s}}{210 \text{ MeV}}\right]^2 \left[\frac{|V_{ts}|}{0.040}\right]^2 \left[\frac{\overline{m_t}(m_t)}{170 \text{ GeV}}\right]^{3.12} \quad (3.1)$$

We have denoted the running top mass with a bar, $\overline{m_t}$.

3.3 $B_{s,d} \to \ell^+ \ell'^-$ in a 2HDM

$B_{s,d} \to \ell^+ \ell'^-$ has also been studied for general two Higgs doublet models (2HDM). Hewett, Nandi, and Rizzo [24], He, Nguyen, and Volkas [25], and Logan and Nierste [26] identified the importance of $\tan\beta$ in producing an excess over Standard Model predictions in this decay rate. The branching ratio in the general 2HDM case is enhanced by the fourth power of $\tan\beta$. This carries over to the MSSM case, but we shall see in the next section that the structure of the MSSM allows an even further enhancement. Logan and Nierste give the following form for the $B_s^0 \to \mu^+ \mu^-$ decay:

$$\begin{aligned} \mathrm{Br}\left(B_s^0 \to \mu^+ \mu^-\right) &= 1.1 \times 10^{-5} \left[\frac{\tau_{B_s}}{1.54 \text{ ps}}\right] \left[\frac{f_{B_s}}{245 \text{ MeV}}\right]^2 \left[\frac{|V_{ts}|}{0.040}\right]^2 x^2 \sqrt{f(x)} \\ &\quad \times \left\{ f(x)\, g(y,z)^2 + [g(y,z) - Y(m_t)]^2 \right\}, \end{aligned} \quad (3.2)$$

with the following function definitions,

$$f(x) = 1 - 4x^2 \quad (3.3)$$

$$g(y,z) = y^2 \frac{\log z}{z-1} \quad (3.4)$$

$$Y(m_t) = 0.997 \left[\frac{\overline{m_t}(m_t)}{166 \text{ GeV}}\right]^{1.55}, \quad (3.5)$$

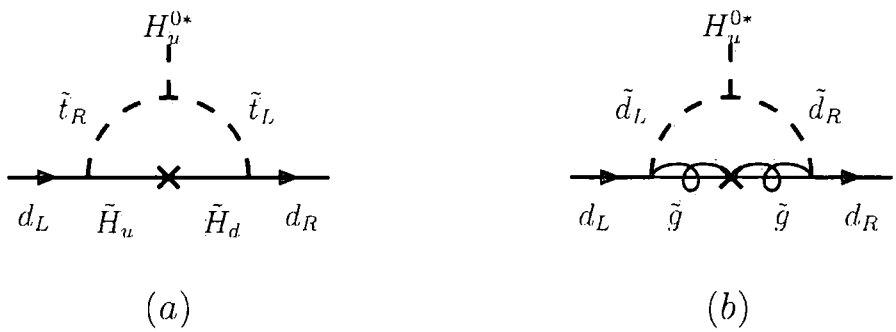

Figure 3.3: One-loop contributions to the H_u coupling with down quarks (a) via Higgsinos and (b) via gluinos which can lead to FCNCs. Flavour indices are suppressed.

and the following variable definitions,

$$x = \frac{m_\mu}{m_{B_s}} \tag{3.6}$$

$$y = \frac{m_{B_s}}{2\sqrt{2}M_W} \tan\beta \tag{3.7}$$

$$z = \frac{m_{H^+}^2}{\overline{m}_t^2(m_t)}. \tag{3.8}$$

3.4 $B_{s,d} \to \ell^+ \ell'^-$ in the MSSM with large $\tan\beta$

In the case of the MSSM, Hall, Rattazzi, and Sarid showed that there are further $\tan\beta$ enhancements from the non-holomorphic QDH_d operator [27]. Blazek, Raby, and Pokorski then showed explicitly the effect of large $\tan\beta$ on the CKM matrix [28]. In a generic Type II 2HDM the two Higgses are sequestered into different Yukawa couplings; namely H_u couples to up-type quarks while H_d couples to down-type quarks and leptons. Indeed, the MSSM superpotential we wrote in equation (2.12) does this manifestly. However, the additional structure of the MSSM circumvents this sequestering at the one-loop level. Diagrams contributing to the H_u coupling to down quarks are illustrated in Figure 3.3. The neutral component of the H_u^a doublet is H_u^2. For simplicity we work in the unbroken $SU(2)_L \times U(1)_Y$ basis, so that the charged Higgsinos in diagram (a) are, in the broken basis, charginos. Note that diagram (b) is permitted because of the nonholomorphic terms in the soft SUSY-breaking Lagrangian of equation (2.13). The holomorphy of the superpotential protects the Type II 2HDM sequestering, but the additional structure of the nonholomorphic terms and the charginos evade this.

The appearance of a loop-level coupling of the down quarks to the up-type neutral Higgs generates a term in the effective Lagrangian for the down quark Yukawas,

$$\mathcal{L}_Y^{\text{one-loop}} \supset H_u^{2*} \overline{d_R} \mathbf{y_d} \left(\epsilon_g + \epsilon_u \mathbf{a_u^\dagger y_u}\right) d_L, \tag{3.9}$$

where the factors ϵ_g and ϵ_u contain couplings and kinematic factors,

$$\epsilon_g \simeq \frac{2\alpha_s}{3\pi} M_3 f(M_3^2, m_{\tilde{Q}}^2, m_{\tilde{d}}^2) \tag{3.10}$$

$$\epsilon_u \simeq \frac{1}{16\pi^2} \mu^* f(\mu^2, m_{\tilde{Q}}^2, m_{\tilde{u}}^2). \tag{3.11}$$

The function f comes from performing the loop integral and is given by [29, 30]

$$f(x,y,z) = -\frac{xy\ln(\frac{x}{y}) + yz\ln(\frac{y}{z}) + xz\log(\frac{z}{x})}{(x-y)(y-z)(z-x)}. \tag{3.12}$$

It was shown by Babu and Kolda [30], Choudhury and Gaur [31], and Huang, Wei, Yan, and Zhu [32] that this new structure can give rise to significant flavour-violating effects in the regime of large $\tan\beta$. In particular, the process $B_{s,d} \to \ell^+ \ell'^-$ is enhanced by powers of $\tan\beta$. Let us show this heuristically following the approach of Kane, Kolda, and Lennon[4] [33].

For simplicity, let us work in the basis where the tree-level down-type Yukawa matrices are diagonal, i.e. where the CKM matrix has been shifted to the up-quark sector. Further, let us only consider the two heaviest down-type quarks so that the diagrams in Figure 3.3 contain an incoming s_L quark and an outgoing b_R quark. We shall ignore the gluino contribution in Figure 3.3b since it will not produce leading-order enhancements in $\tan\beta$, and for further simplicity we shall only consider the case $\mathbf{a_u} = a_u \mathbf{y_u}$. The large $\tan\beta$ dependence derived from this simplified case is identical to the general case. In this approximation, the $s_L b_R H_u^{2*}$ coupling of Figure 3.3a takes the form $y_b y_t^2 V_{is} a_u \epsilon_u$, where y_t is the top quark Yukawa and we have used the fact that in the basis where the down-type Yukawas are diagonal, the up-type Yukawas are proportional to the CKM matrix, $\mathbf{V}$.

[4] We follow the argument first four pages of [33], taking the liberty to fix some of its typos.

Upon electroweak symmetry breaking, the effective mass term between the two heaviest down-type quarks then takes the form

$$\mathcal{L}_{\text{mass}}^{\text{one-loop}} \supset \begin{pmatrix} \bar{s}_R & \bar{b}_R \end{pmatrix} \begin{pmatrix} m_s & 0 \\ y_b \epsilon v_u & m_b \end{pmatrix} \begin{pmatrix} s_L \\ b_L \end{pmatrix}, \tag{3.13}$$

where we have written $\epsilon = y_t^2 V_{is} a_u \epsilon_u$. This means that the one-loop masses are diagonalised by rotating the down-quarks in the $s_L - b_L$ plane by an angle $\sin\theta \simeq y_b \epsilon v_u / m_b$. Using the relations $m_b = y_b v_d$ and $\tan\beta \equiv v_u/v_d$, we find

$$\sin\theta \simeq \epsilon \tan\beta. \tag{3.14}$$

Now consider the amplitude $\mathcal{M}_{s'\bar{b}\to\ell\bar{\ell}}$ for dilepton B_s^0 decay in the one-loop mass eigenbasis (denoted by the prime on the s quark). We shall neglect the one-loop FCNC effects on the b quark for simplicity ($b' \approx b$) and expand the one-loop strange quark eigenstate into it's tree-level mass eigenstates:

$$\mathcal{M}_{s'\bar{b}\to\ell\bar{\ell}} = \cos\theta \left(\mathcal{M}_{s\bar{b}\to\ell\bar{\ell}}\right) + \sin\theta \left(\mathcal{M}_{b\bar{b}\to\ell\bar{\ell}}\right). \tag{3.15}$$

The second term on the right hand side is enhanced by a power of $\tan\beta$ from the $\sin\theta$ and by two additional powers of $\tan\beta$ from the y_b and y_μ vertices at tree level, as shown in Figure 3.4. This is because the down and lepton Yukawa couplings take the form

$$y_{b,\ell} = \frac{m_{b,\ell}}{v_d} \propto \frac{1}{\cos\beta}. \tag{3.16}$$

In the limit of large $\tan\beta$, however, $1/\cos\beta \to \tan\beta$. Hence the leading-order diagrams in $\tan\beta$ for $s\bar{b} \to \mu\mu$ is enhanced by three powers of $\tan\beta$. These factors can overwhelm the loop suppression factor ϵ in the large $\tan\beta$ regime, causing the branching ratio to be dominated by the neutral Higgs penguins.

This regime has generated a lot of interest since the large $\tan\beta$ (~ 50) scenario is preferred by grand unified models where the hierarchy between the top and bottom masses are explained by a large difference in the Higgs vevs, hence allowing unification of the Yukawa couplings. The 2σ signal of an excess in the anomalous magnetic moment of the muon $(g-2)_\mu$ is also suggestive of a large $\tan\beta$ in certain supersymmetric models, such as mSUGRA [34]. The upside is that the $\tan^6\beta$ enhancement in this region pushes

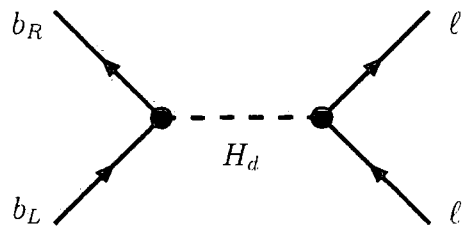

Figure 3.4: Tree-level contribution to $\mathcal{M}_{b\bar{b}\to\ell\bar{\ell}}$ in the tree-level mass eigenbasis. The vertices give factors of y_b and y_ℓ respectively.

the MSSM signal above the suppressed Standard Model prediction from section 3.1.3, making $B_s^0 \to \mu^+ \mu^-$ a mode with a high discovery potential.

However, because the effective Yukawa coupling between the down quark and the up-type Higgs depends on $\tan\beta$, one must be careful about the validity of perturbation theory in the large $\tan\beta$ regime. To this end a method to resum the $\tan\beta$-enhanced couplings was developed by Dedes and Pilaftsis [35] and Buras, Chankowski, Rosiek, and Slawianowska [36]. The latter of which cite the branching ratio for the phenomenologically interesting decay $B_s^0 \to \mu^+ \mu^-$ in the large $\tan\beta$ limit to be

$$\begin{aligned} \mathrm{Br}\left(B_s^0 \to \mu^+ \mu^-\right) &= 3.5 \times 10^{-5} \left[\frac{\tan\beta}{50}\right]^6 \left[\frac{\tau_{B_s}}{1.5\ \mathrm{ps}}\right] \left[\frac{f_{B_s}}{230\ \mathrm{MeV}}\right]^2 \left[\frac{|V_{ts}|}{0.040}\right]^2 \\ &\quad \times \frac{m_t^4}{M_A^4} \frac{(16\pi^2 \epsilon_u a_u y_t^2)^2}{(1 + (\epsilon_g + \epsilon_u a_u y_t^2)\tan\beta)^2 (1 + \epsilon_g \tan\beta)^2}. \end{aligned} \tag{3.17}$$

Here τ_{B_s} and f_{B_s} as the B_s^0 lifetime and decay constant. Here only the Wilson coefficients proportional to $\tan^3\beta$ are taken, with the assumption that $M_{H^0}^2 \approx M_{A^0}^2$. To ease comparison we have assumed[5] that $\mathbf{a_u} = a_u \mathbf{y_u}$. The 'large $\tan\beta$' assumption is valid for $\tan\beta \gtrsim 30$, with SUSY contributions approaching the Standard Model order of magnitude for $\tan\beta \lesssim 10$ [37]. We shall also implicitly include small M_A as part of the 'large $\tan\beta$' assumption.

[5]Buras *et al.* do not restrict themselves to this assumption, but this limit eases the comparison with our definition of the ϵ terms as well as those in the non-resummed analysis by Isidori and Retico [37].

3.5 $B_{s,d} \to \ell^+ \ell'^-$ in the MSSM with small $\tan\beta$

At the eve of the LHCb era of B physics, it is timely to do a complete analysis of the $B_s^0 \to \mu^+ \mu^-$ for arbitrary $\tan\beta$. Indeed, this is one of the 'benchmark' decay modes for the LHCb in part because of the aforementioned sensitivity to new physics. Such a study was conducted by Chankowski and Slawianowska [38] prior to the development of the resummation techniques, but it focused on the early discovery potential of the large $\tan\beta$ regime.

What remainds to be properly understood are the less favourable regions of parameter space in the specific context of the LHCb's discovery potential. In particular, we would like to plot out the parameter space for possible 'nightmare scenarios' where $\mathrm{Br}(B_s^0 \to \mu^+ \mu^-)$ is below the discovery threshold of the LHCb. In other words, we would like to understand how coy nature could be in this decay channel. The LHCb will be able to probe just past the Standard Model branching ratio prediction. A plot of LHCb sensitivity versus integrated luminosity is provided in Figure 3.5. If the decay rate is beyond this sensitivity, we would like to quantitatively understand what this might tell us about supersymmetric models. This is the B physics analog to the recent phenomenological interest in Higgsless models with an eye for 'nightmare scenarios' at the LHC general purpose detectors (ATLAS and CMS) where a Higgs is not discovered.

Further motivation for a broader scan of parameter space comes from recent 'beyond minimal flavour violation' model-buliding efforts. Two such studies are those by Nomura, Papucci, and Stolarski [40] and Feng, Lester, Nir, and Shadmi [41]. Both advocate the hope that nontrivial flavour structure may still be lurking in the MSSM.

In this study, we would like to focus on the effects of the *small* $\tan\beta$ (and implicitly large M_A) regime as part of a larger project to develop publically available code for a completed, resummed calculation over all of the viable parameter space for $B_{s,d} \to \ell^+ \ell'^-$ [1]. We shall here focus on the low $\tan\beta$ regime where the Higgs penguins are suppressed and the box and Z penguins dominate. We shall also mention the intermediate region where all of the above diagrams are of the same order of magnitude. This is particularly interesting because the quantum interference between these diagrams can lead to potential cancellations and a dip in the overall branching ratio.

If the branching ratio for $B_{s,d} \to \ell^+ \ell'^-$ is well below the Standard Model prediction, the signal for new physics in this channel might be a *non-signal* at the LHCb. In this case

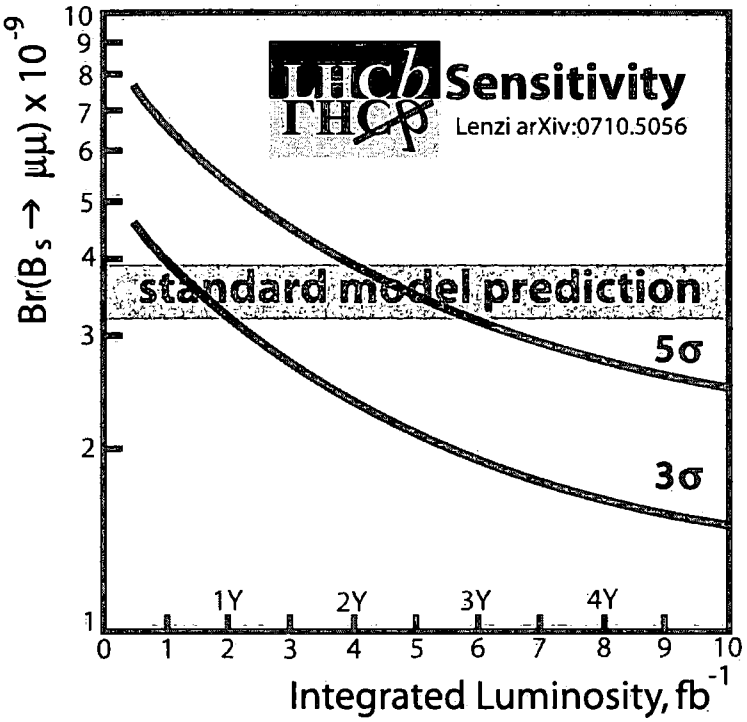

Figure 3.5: LHCb sensitivty to $B_s^0 \to \mu^+ \mu^-$, adapted from [39].

we may turn to current plans for an LHCb upgrade in the next decade [42], but we must first understand the parameter space of our models before making key decisions about how to upgrade the machine. For example, depending on the lower-bound of the MSSM prediction for $B_{s,d} \to \mu^+ \mu^-$, it may be more strategic to increase luminosity around the $B_s^0 \to \mu^+ \mu^-$ Standard Model expectation rather than reaching for the Standard Model expectation for the $B_d^0 \to \mu^+ \mu^-$ branching ratio.

Chapter 4

Calculating $B_{s,d} \to \ell^+ \ell'^-$

"Shut up and calculate!"
— R. Feynman (apocryphal)

In this chapter we go over the calculation of the branching ratio $\mathrm{Br}\left(B_{s,d} \to \ell^+ \ell'^-\right)$ in Wilsonian effective field theory. This summarises the bulk of the calculational work done on the project. We begin with a brief description of the effective field theory paradigm and then explain its application to the decay $B_{s,d} \to \ell^+ \ell'^-$. We close with some words on computational aspects of programming this calculation for numerical results over parameter space.

Our description of effective field theory is based on the effective field theory review article by Georgi [13], the weak decay review article by Buchalla, Buras, and Lautenbacher [14] and the review of heavy flavour physics by Buras [15].

4.1 Effective field theory overview

The goal of Wilsonian effective field theory (EFT) is to understand how a theory at a particular energy scale changes as one integrates out much heavier degrees of freedom. In this way one is able to isolate the relevant physics at the particular energy scale and greatly simplify calculations.

A heuristic example is Newtonian mechanics, which is still taught to school children even though it is only the low-energy 'effective theory' of special relativity, or further still of general relativity. Slightly more formally, an effective field theory is obtained by taking the masses of heavy particles of a 'full theory' to infinity, or alternately taking the length scales of the associated physics to zero. In doing this, one implicitly introduces a renormalisation scale and running coupling. Essentially one has traded the logarithmic dependence on heavy particle masses in a full theory for a scale dependence of the generally nonrenormalisable effective theory[1].

The key idea is that the physics at a given energy scale shouldn't be too sensitive to—i.e. should *decouple* from—physics at a much higher energy scales. The Wilsonian programme makes this decoupling explicit by working with an **effective Hamiltonian** of the form

$$\mathcal{H}_{\text{eff}} = \sum_i C_i(\mu, Q)\mathcal{O}_i(\mu). \tag{4.1}$$

The $\mathcal{O}_i$ are effective local operators that represent the low-energy effective theory while the C_i are Wilson coefficients that encode the relevant information from the high scale theory. Q is the matching scale at which the high-energy 'full theory' is patched onto the low-energy theory. It represents the "cutoff" at which the effective field theory breaks down, i.e. M_W. Finally, μ is the renormalisation scale that separates the high and low scales of the EFT by separating how the information of the running from Q is divided between the renormalisation of the operators and Wilson coefficients. Formally this is just an operator product expansion where nonlocal operators, such as those with a propagating heavy particle, are replaced by a series of local effective operators. The amplitude for a given process is then

$$\mathcal{M} = \langle \mathcal{H}_{\text{eff}} \rangle = \sum_i C_i(\mu, Q)\langle \mathcal{O}_i(\mu) \rangle. \tag{4.2}$$

Up to this point the EFT approach may seem to only be calculational convenience. For the weak decays of mesons, however, effective field theory is a calculational necessity. Mesons are bound states of strongly coupled quarks and gluons, and hence are inherently

[1]The intimate relation to the renormalisation group is not coincidental. When we renormalise in the Standard Model, we are acknowledging that the Standard Model is itself only an effective field theory of some unknown higher-scale physics. Georgi labels this point of view 'continuum effective field theory' to differentiate from the 'Wilsonian effective field theory' we describe here [13]. The naming is somewhat irrelevant, however, as these are just two sides of the same coin: high-scale physics is decoupled from low-scale physics.

quantum chromodynamic objects. The details of the QCD that binds the meson together at low energies is inescapably nonperturbative, making 'full' Standard Model calculations of mesonic interactions intractable by usual methods.

However, for the weak (i.e. non-chromodynamic) decays of mesons, one is not interested in the details of the 'high-energy' quark-gluon picture. Effective field theory allows us to work with a perturbative theory of only the component quarks. For rare (semi)leptonic decays, we are often able to completely encode 'high-scale' QCD effects into form factors and decay constants that can be determined either by experiment or lattice techniques. We shall see that the decays $B_{s,d} \to \ell^+ \ell'^-$ are particularly nice in this respect since all hadronic uncertainties can be represented by a single number. The renormalisation of the effective theory is not problematic, since $\alpha_s(\mu)$ is a reasonable perturbation expansion parameter above $\mathcal{O}(1\text{ GeV})$. We shall perform the calculation for the decay $B_s^0 \to \ell^+ \ell'^-$. The analogous calculation for $B_d^0 \to \ell^+ \ell'^-$ is found by trivially replacing $s \to d$.

The EFT programme for weak decays of mesons can be summarised in these steps:

1. Identify the matching scale Q, renormalisation scale μ, and the effective operators $\mathcal{O}_i$ in the low-energy regime.
2. Calculate the Wilson coefficients at the scale Q by matching the high-scale theory to the effective theory.
3. Use the renormalisation group to run the effective operators from the matching scale to the 'experiment' (mesonic) scale.
4. Calculate hadronic matrix elements at the low-scale using some nonperturbative method.

The last step usually involves 'taking a result off the shelf' from, for example, lattice QCD calculations. We shall see that in $B_{s,d} \to \ell^+ \ell'^-$ we can perform this last step immediately since the hadronic matrix elements take a particularly simple form. We shall match and renormalise at the weak scale, $Q = \mu = M_W$, hence the renormalisation group equations are simply those of the Standard Model.

4.2 Effective Operators

Let us now apply this EFT approach to the decay $B_{s,d} \to \ell^+ \ell'^-$. A schematic decomposition into box, vector penguin, and scalar penguin 'blob' diagrams is shown in Figure

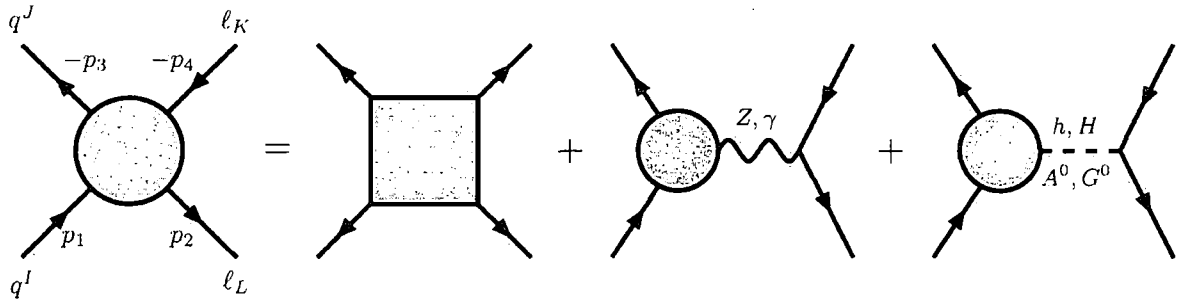

Figure 4.1: Generic box and penguin diagrams contributing to $B_{s,d} \to \ell^+ \ell'^-$ with our index and momentum conventions.

4.1. We shall label our external fermions with capital Roman indices I, J, K, L, so that the decay $B_s^0 \to \mu^+ \mu^-$ would correspond to $q^J = b$, $q^I = s$, $\ell^K = \mu$, $\ell^L = \mu$, following the definition of the B_s^0 meson in Section 3.1.2.

There are three scales in this process. The supersymmetry breaking scale M_{SUSY} represents the scale at which gluinos are 'integrated out' and become inactive. Hence below this scale we may ignore their effects on the QCD running and use the Standard Model QCD renormalisation group flow. We take our matching scale to be the top mass $Q = m_t$, hence the renormalisation down to the B_s^0 scale won't require further QCD matching between numbers of active flavours. The renormalisation scale μ may be taken arbitrarily for now, as we shall show that our amplitude will be a renormalisation group invariant.

Our low-energy effective operators given by

$$\begin{aligned} \mathcal{O}^V_{XY} &= \overline{q^J} \gamma^\mu P_X q^I \otimes \overline{\ell^L} \gamma_\mu P_Y \ell^K \\ \mathcal{O}^S_{XY} &= \overline{q^J} P_X q^I \otimes \overline{\ell^L} P_Y \ell^K \\ \mathcal{O}^T_X &= \overline{q^J} \sigma^{\mu\nu} P_X q^I \otimes \overline{\ell^L} \sigma^{\mu\nu} P_Y \ell^K . \end{aligned} \tag{4.3}$$

where $X, Y \in L, R$ label chirality and V, S, T label vector, scalar, and tensor operators respectively. $P_{L,R} = \frac{1}{2}(1 \mp \gamma_5)$ are the chiral projection operators. This complete basis of ten operators explicitly captures the factorisation between hadronic and leptonic matrix elements that we will exploit in Section 4.3. A diagrammatic representation of these operators is given in Figure 4.2. At this point, however, one might express some concern over diagrams where quark and lepton spinor structures are connected, such as those in

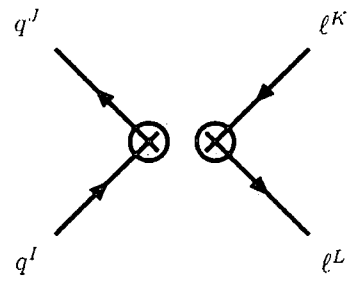

Figure 4.2: Diagrammatic form of the effective operators in equation (4.3).

Figure 4.5. These, however, can be expressed in terms of the above basis using Fierz identities. These identities are reproduced for reference in Appendix C.

We shall normalise our coefficients[2] so that the effective Hamiltonian is given by

$$\mathcal{H} = \frac{1}{(4\pi)^2} \sum_{X,Y=L,R} \left(C^V_{XY} \mathcal{O}^V_{XY} + C^S_{XY} \mathcal{O}^S_{XY} + C^T_X \mathcal{O}^T_X \right). \tag{4.4}$$

The diagrams contributing to these coefficients are shown below in Section 4.6. We list contributions to each Wilson coefficient $\left(C^Z_{XY}\right)_i$, where i labels the contribution from a particular diagram, in Appendix E. The full coefficient is given by the sum of each contribution,

$$C^Z_{XY} = \sum_i \left(C^Z_{XY}\right)_i. \tag{4.5}$$

4.3 Simplification by factorisation

The decay amplitude for $B_{s,d} \to \ell^+ \ell'^-$ factorises between the hadronic initial state and the leptonic final state:

$$\langle \ell, \ell' | \mathcal{H}_{\text{eff}} | B^0_s(p) \rangle = \sum_{i=\text{ops}} \langle \ell, \ell' | \mathcal{O}^i_L | 0 \rangle \langle 0 | \mathcal{O}^i_Q | B^0_s(p) \rangle. \tag{4.6}$$

On the left hand side of this equation is the amplitude for the decay, where $\mathcal{H}_{\text{eff}}$ is the effective Hamiltonian. On the right hand side is a sum over the product of amplitudes between the external states and the vacuum with respect to effective operators in the

[2]This normalisation is a relic of the standard definition of the loop integrals with a leading factor of $1/(4\pi)^2$. See Appendix D.2.

hadronic and leptonic sectors. This decomposition can be understood by noting that the terms in the Standard Model Lagrangian that mediate this decay don't mix quarks with leptons. Hence the effective Hamiltonian contains terms of the form $\mathcal{O}_L \mathcal{O}_Q$ one can insert a complete set of intermediate states between these operators. Since the hadronic in-states fully contract the $\mathcal{O}_Q$ operators and the leptonic out-states fully contract the $\mathcal{O}_L$ operators, only the ground state contributes in the set of intermediate states. Summing over the effective operators, one finds the factorisation of equation (4.6).

Let us now focus on the hadronic amplitudes on the right hand side. Consider the relevant vector operator $\left(\mathcal{O}_Q^V\right)_{L,R} = \bar{b}\gamma_\mu P_{L,R} s$. By Lorentz covariance and because the only object available to use as a four-vector is the momentum of the B meson, p, we can constrain the form of the hadronic amplitude to be

$$\langle 0|\bar{b}\gamma_\mu P_{L,R} s|\mathrm{B_s^0}(p)\rangle = \mp\frac{i}{2} p_\mu f_{B_s}. \tag{4.7}$$

This equation defines the decay constant f_B of the $\mathrm{B_s^0}$ meson. This is a number that fully incorporates the nonperturbative physics of the QCD bound state. It is calculated via lattice methods. We can go further and contract equation (4.7) with p_μ.

$$\langle 0|\bar{b}\,\not{p}\, P_{L,R} s|\mathrm{B_s^0}(p)\rangle = \mp\frac{i}{2} M_{B_s} f_B \tag{4.8}$$

$$\langle 0|\bar{b}\,(\not{p}_b + \not{p}_s)\, P_{L,R} s|\mathrm{B_s^0}(p)\rangle = \mp\frac{i}{2} M_{B_s} f_B. \tag{4.9}$$

Here we've dropped a term representing the momentum carried by virtual quarks and gluons, $\not{p}_{\mathrm{QCD}}$ since we expect this to be on the order of $\mathcal{O}(100\ \mathrm{MeV}) \ll m_b$. We can now apply the quark equations of motion. To do this explicitly, we may Wick contract the creation and annihilation operators in the matrix element to find

$$\begin{aligned}
\langle 0|\bar{b}\,(\not{p}_b + \not{p}_s)\, P_{L,R} s|\mathrm{B_s^0}(p)\rangle &= \overline{v}(p_b)\,(\not{p}_b + \not{p}_s)\, P_{L,R}\, u(p_s) && (4.10)\\
&= -m_b\, \overline{v}(p_b)\, P_{L,R}\, u(p_s) + m_s \overline{v}(p_b)\, P_{R,L}\, u(p_s) && (4.11)\\
&= -(m_b + m_s)\, \overline{v}(p_b)\, P_{L,R}\, u(p_s) + m_s \overline{v}(p_b) u(p_s) && (4.12)\\
&= -(m_b + m_s)\langle 0|\bar{b} P_{L,R} s|\mathrm{B_s^0}(p)\rangle. && (4.13)
\end{aligned}$$

Here we've used $P_L + P_R = \mathbb{1}$ and the orthogonality of the plane wave spinors $\overline{v}(p)u(k) \equiv 0$. Hence we may write the matrix element for the *scalar* operators as

$$\langle 0|\bar{b} P_{L,R} s|\mathrm{B_s^0}(p)\rangle = \pm\frac{i}{2}\frac{M_{B_s} f_B}{m_b + m_s}. \tag{4.14}$$

We have now written the vector and scalar hadronic matrix elements in terms of the decay constant and various masses, i.e. in terms of an overall coefficient.

We can go even further to simplify the matrix element. The matrix element for hadronic tensor operator $\langle 0|\bar{b}\sigma_{\mu\nu}s|\mathrm{B}_s^0(p)\rangle$ vanishes explicitly since there is no way to create an antisymmetric tensor out of a single momentum p_μ. Next, the photon penguin vanishes since it is proportional to

$$\langle \ell, \ell'|\overline{\ell'}\gamma_\mu P_Y \ell|0\rangle\langle 0|\bar{b}\gamma^\mu P_X s|\mathrm{B}_s^0(p)\rangle \propto p^\mu \langle \ell, \ell'|\overline{\ell'}\gamma_\mu P_Y \ell|0\rangle,$$

which vanishes by the Ward identiy (i.e. conservation of the electromagnetic current).

4.4 Branching Ratio

We can now write the amplitude in terms of only leptonic operators:

$$\mathcal{M} = F_S \bar{\ell}\ell + F_P \bar{\ell}\gamma_5 \ell + F_V p^\mu \bar{\ell}\gamma_\mu \ell + F_A p^\mu \bar{\ell}\gamma_\mu\gamma_5 \ell, \tag{4.15}$$

where the (S)calar, (P)seudovector, (V)ector, and (A)xial-vector form factors F are given by

$$\begin{aligned}
F_S &= \frac{i}{4}\frac{M_{B_s}^2 f_{B_s}}{m_b + m_s}\left(C_{LL}^S + C_{LR}^S - C_{RR}^S - C_{RL}^S\right), \\
F_P &= \frac{i}{4}\frac{M_{B_s}^2 f_{B_s}}{m_b + m_s}\left(-C_{LL}^S + C_{LR}^S - C_{RR}^S + C_{RL}^S\right), \\
F_V &= -\frac{i}{4} f_{B_s}\left(C_{LL}^V + C_{LR}^V - C_{RR}^V - C_{RL}^V\right), \\
F_A &= -\frac{i}{4} f_{B_s}\left(-C_{LL}^V + C_{LR}^V - C_{RR}^V + C_{RL}^V\right).
\end{aligned} \tag{4.16}$$

Note that we have changed our basis of operators from the chiral basis of equation (4.3) to a basis where the Lorentz transformation properties are manifest. The diagrammatic contributions to the Wilson coefficients are discussed in Section 4.6 below.

Performing the kinematic integrals, the branching ratio for a scalar particle decaying into two spin-1/2 particles is given in terms of the matrix element $\mathcal{M}$ by

$$\mathrm{Br}(B_s^0 \to \ell\ell') = \frac{\tau_B}{16\pi}\frac{|\mathcal{M}|^2}{M_B}\sqrt{1-\left(\frac{m_\ell + m_{\ell'}}{M_B}\right)^2}\sqrt{1-\left(\frac{m_\ell - m_{\ell'}}{M_B}\right)^2}, \quad (4.17)$$

where τ_B is the B_s^0 lifetime. Squaring the matrix element of equation (4.15), one finds

$$\begin{aligned}
|\mathcal{M}|^2 &= 2|F_S|^2\left[M_{B_s}^2 - (m_{\ell_L} + m_{\ell_K})^2\right] + 2|F_P|^2\left[M_{B_s}^2 - (m_{\ell_L} - m_{\ell_K})^2\right] \\
&+ 2|F_V|^2\left[M_{B_s}^2(m_{\ell_K} - m_{\ell_L})^2 - (m_{\ell_K}^2 - m_{\ell_L}^2)^2\right] \\
&+ 2|F_A|^2\left[M_{B_s}^2(m_{\ell_K} + m_{\ell_L})^2 - (m_{\ell_K}^2 - m_{\ell_L}^2)^2\right] \\
&+ 4\,\mathrm{Re}(F_S F_V^*)(m_{\ell_L} - m_{\ell_K})\left[M_{B_s}^2 + (m_{\ell_K} + m_{\ell_L})^2\right] \\
&+ 4\,\mathrm{Re}(F_P F_A^*)(m_{\ell_L} + m_{\ell_K})\left[M_{B_s}^2 - (m_{\ell_L} - m_{\ell_K})^2\right] . \quad (4.18)
\end{aligned}$$

Note that the contribution of the vector amplitude F_V vanishes in the lepton flavour conserving case $L = K$. In this limit the above result agrees with the publish result by Bobeth *et al.* [16].

4.5 QCD corrections

We now analyse the renormalisation group flow from the matching scale down to to the renormalisation scale μ. Because electroweak corrections are negligibly small in this regime, we only need to consider the QCD renormalisation of the form factors in equation (4.16). These form factors encode all the information about the QCD-sensitive part of the amplitude. The one-loop diagrams contributing to this renormalisation are shown in Figure 4.3. As QCD is blind to the leptonic legs of the effective operators, this is just the renormalisation of a two-point function in QCD. In particular, we note that the Wilson coefficients C_{XY}^S of the scalar operators $\mathcal{O}_{XY}^S$ in equation (4.3) renormalise as quark mass terms,

$$m(\mu^2) = m(Q^2)\exp\left[-\int_{\alpha_S(Q^2)}^{\alpha_S(\mu^2)} d\alpha_S \frac{\gamma_m(\alpha_S)}{\beta(\alpha_S)}\right], \quad (4.19)$$

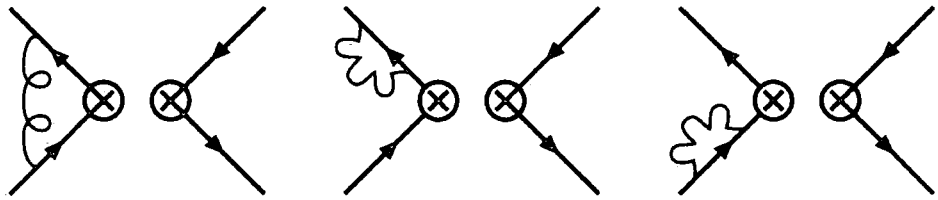

Figure 4.3: One-loop gluon diagrams renormalising the effective operators represented in Figure 4.2.

where γ_m is the anomalous dimension and β is the QCD beta function. The important feature is that this is an overall multiplicative factor. Thus the combination

$$\frac{C^S_{XY}(Q)}{m_b(Q) + m_s(Q)}$$

is invariant under the renormalisation group, and the scalar and pseudoscalar form factors $F_{S,P}$ of equation (4.16) does not renormalise.

Further, the Wilson coefficients C^V_{XY} of the scalar operators $\mathcal{O}^V_{XY}$ are protected by the Ward identy associated with the conservation of the vector-axial current. Hence these operators have vanishing anomalous dimensions and the vector and pseudovector form factors $F_{S,P}$ of equation (4.16) do not renormalise either.

Hence the form factors are renormalisation group invariants and are independent of the renormalisation scale μ, as promised earlier.

We use this freedom to calculate all parameters in equations (4.16) and (4.18) at the scale of the top mass, $Q = m_t$. We calculate SUSY corrections in the $\overline{DR}$ renormalisation scheme [17]. The quark pole masses $m_{b,t}$ are related to the $\overline{DR}$ running masses $m_{b,t}(Q)$ using the formulae

$$m_b(Q) = m_b \left[1 - \frac{5\alpha_S(m_b)}{3\pi}\right] \left[\frac{\alpha_s(Q)}{\alpha_S(m_b)}\right]^{\frac{4}{b_0}} \tag{4.20}$$

$$m_t(m_t) = m_t \left[1 - \frac{5\alpha_s(m_t)}{3\pi}\right], \tag{4.21}$$

where $b_0 = 11 - 2n_f/3$ and the number of effective quarks in the first equation is $n_f = 5$. The initial conditions for parameters have to be converted into the $\overline{DR}$ scheme, the $\overline{MS} \to \overline{DR}$ conversion factor is included in equations (4.20) and (4.21) [18]. We neglect the small effects from the conversion of gauge couplings beween the schemes.

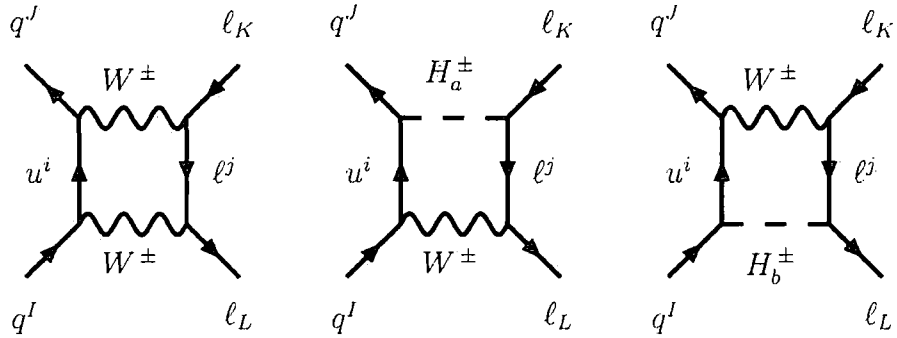

Figure 4.4: Box diagrams without Majorana fermions.

4.6 Diagrams and matching

We now show the MSSM diagrams that contribute to the Wilson coefficients. The results for each diagram are listed explicitly in Appendix E. We shall focus on the low $\tan\beta$ regime and hence neglect the effect of the suppressed neutral Higgs diagrams and instead focus on the box and Z penguins.

The box diagrams without Majorana fermions are shown in 4.4. These diagrams are the same as those in a minimal Type II 2HDM.

In addition, there are the box diagrams shown in Figure 4.5 containing Majorana fermions. These fermions are gauginos that come from 'supersymmetrising' the 2HDM boxes above. Note that conventional Feynman rules cannot be used for the fermion number violating Majorana interactions. Instead we use the conventions of Denner *et al.* from [49] and [50]. These boxes also generate a different spinor structure that's not automatically factorised. As noted above, one must apply the Fierz identities (reproduced in Appendix C) to rearrange the resulting operators into those in equation (4.3).

Finally, we list the contributions to the Z-penguins. The full contribution to the $B_{s,d} \to \ell^+ \ell'^-$ amplitude is recovered by multiplying the penguin amplitude by

$$\frac{1}{M_Z^2} \frac{e(1-\sin^2\theta_W)}{2\sin\theta_W \cos\theta_W} \; \bar{\ell}^L \gamma_\mu P_L \ell^K.$$

The 1PI contributions are given in 4.6.

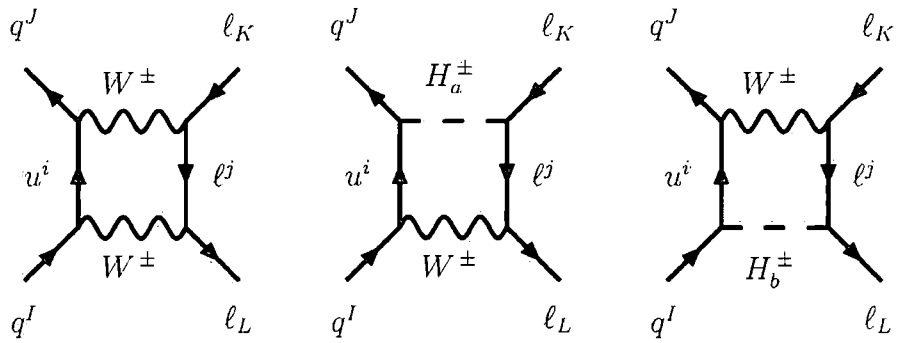

Figure 4.5: Box diagrams with Majorana fermions.

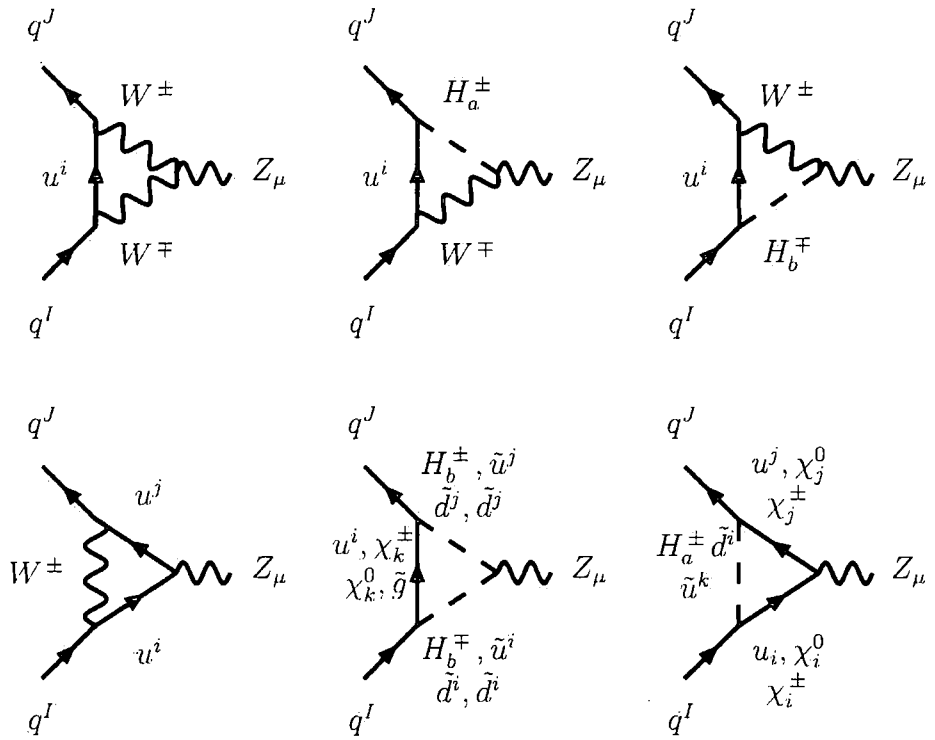

Figure 4.6: 1PI Z-penguin diagrams.

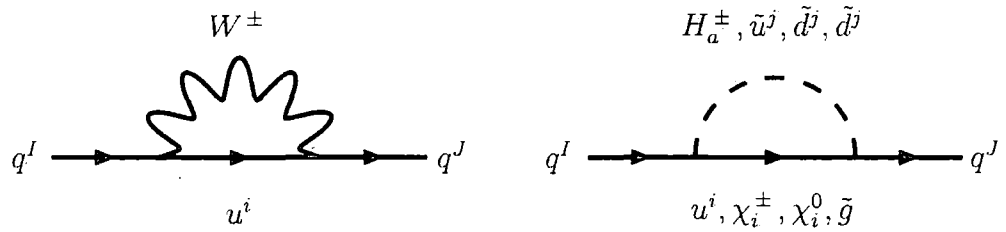

Figure 4.7: FCNC self-energy diagrams.

In addition to the 1PI diagrams, there are flavour-changing down-quark self-energy diagrams shown in 4.7. Each diagram can be inserted into the q^I or the q^J legs and hence represent two Z-penguin topologies.

4.7 Computational approach

This calculation is part of a larger project to develop a computer program to calculate the full, resummed $B_{s,d} \to \ell^+ \ell'^-$ branching ratio across all of parameter space to be made available for public use [1]. The code for this low $\tan\beta$ study including only the box and Z-penguins was developed independently as a cross check for a simultaneous effort to incorporate the same calculations into an existing library of MSSM decays [51] previously used in studies of supersymmetric Higgs decays with radiative corrections [52] and K decays [53]. The code was written in Fortran 95. This was chosen for its ease in coding mathematics and backwards compatibility with Fortran 77 code such as that of [51].

The numerical calculation is automated as a function of MSSM input parameters. The reduction of diagrams to effective operators is done by hand in terms of generic vertices, such as those in Appendix E.1. The program then diagonalises the MSSM following the procedure of Appendix B, fills in the appropriate vertices fiven the MSSM input parameters, and calculates the amplitude and branching ratio using the formulae in this chapter.

Scans over parameter space are done by including this code into the existing library in [51] which incorporates all current experimental constrants.

Chapter 5

Physics Results and Conclusions

"And now let's generalise to the case $N = 3$."
— Ben Allanach

We now discuss the results of a scan of the low $\tan\beta$ (and heavy M_A) regime dominated by box and Z-penguin diagrams and point towards future directions and implications for the LHCb physics programme.

5.1 General analysis

We shall focus on the lepton flavour conserving processes $B_{s,d} \to \ell^+ \ell^-$. We shall also take the limit

$$\frac{m_\ell}{M_{B_{s,d}}} \to 0.$$

In this case, the squared amplitude of equation (4.18) reduces to

$$|\mathcal{M}|^2 \approx 2M_{B_{s,d}}^2 \left(|F_S|^2 + |F_P + 2\, m_\ell\, F_A|^2\right). \tag{5.1}$$

We would like to understand the minimum of this function, i.e. the minimum of the decay $B_{s,d} \to \ell^+ \ell^-$. This occurs when $|F_S|^2 = |F_P|^2 = |F_A|^2 = 0$. In the limit of low $\tan\beta$ and large M_A that we're interested in, the SUSY contributions to F_S and F_P are $\tan\beta$ *suppressed* and the dominant effects come from the axial vector contribution F_A. This can be seen by considering the order of magnitude of the Wilson coefficients

in Appendix E using the analytic integral forms of Appendix D.2. The scalar and pseudoscalar operators only contribute from the Standard Model Higgs channels, which results in contributions on the order of

$$\mathrm{Br}\left(\mathrm{B}_{\mathrm{d}}^{0} \to \ell^{+}\,\ell^{-}\right)_{\text{SM Higgs}} \lesssim 10^{-12} \tag{5.2}$$

$$\mathrm{Br}\left(\mathrm{B}_{\mathrm{s}}^{0} \to \ell^{+}\,\ell^{-}\right)_{\text{SM Higgs}} \lesssim 10^{-11}. \tag{5.3}$$

This sets an approximate lower bound on the minimum of $|\mathcal{M}|^2$ as we vary F_A while considering only the box and Z-penguin diagrams. In other words, if our calculation using only the box and Z-penguin diagrams leads to a vanishing F_A, then the branching ratio for the process will be given by the estimated Higgs-mediated branching ratios above.

The question now is to understand how small F_A can become given the experimental constraints from K and B physics.

5.2 Scan of parameter space

In order to answer this question we perform a scan of parameter space using the code in [51] augmented with our calculations. The range of input parameters and the sampling steps are given in Table 5.1. By "SUSY" scale we mean a common mass parameter for the first two squark generations. All mass parameters are in GeV and we have assumed that M_1 is related to M_2 by grand unification boundary conditions.

The mass insertions δ are defined following Gabbiani *et al.* [54], Misiak *et al.* [55], and Buras *et al.* [53]:

$$\delta^{IJ}_{QXY} = \frac{(M^2_Q)^{IJ}_{XY}}{\sqrt{(M^2_Q)^{IJ}_{XX}(M^2_Q)^{IJ}_{YY}}} \tag{5.4}$$

Here I, J denote quark flavours, X, Y denote superfield chirality, and Q indicates either the up or down superfield sector. This is not necessarily an intuitive parameter, so a brief discussion is in order. Recall from Chapter 1 that the flavour strucutre of a theory comes from mass matrices that are not diagonal in flavour space, leading to a tension between interaction eigenstates and propagating eigenstates. Even though we work in

Parameter	Symbol	Min	Max	Step
Ratio of Higgs vevs	$\tan\beta$	2	10	1
CKM phase	γ	$-\pi$	π	$\pi/25$
CP-odd Higgs mass	M_A	100	500	200
SUSY Higgs mixing	μ	-450	450	300
$SU(2)$ gaugino mass	M_2	100	500	200
Gluino mass	M_3	$3M_2$	$3M_2$	0
SUSY scale	M_{SUSY}	200	1000	200
Slepton Masses	$M_{\tilde{\ell}}$	$M_{\text{SUSY}}/3$	$M_{\text{SUSY}}/3$	0
Left top squark mass	$M_{\tilde{Q}_L}$	200	1000	200
Right bottom squark mass	$M_{\tilde{b}_R}$	200	1000	200
Right top squark mass	$M_{\tilde{t}_R}$	150	450	150
Mass insertion	δ^{23}_{dLL}	-1	1	1/30

Table 5.1: Range of input parameters for parameter space.

a basis where we have diagonalised the MSSM mass matrices to the extent possible, it is useful to parasmeterise the nontriviality of the theory's flavour structure though the off-diagonal mass matrix elements. The normalised mass insertion in equation (5.4) represents a two point flavour-changing mass interaction in the flavour basis, which we drew heuristically in Figure 3.1. The mass insertions capture all of the flavour structure relevant to the flavour transition between Q^I and Q^J quarks, where Q is either up- or down-type. In general the mass-insertions may be complex with the phase contributing to CP-violating effects. The process $\mathrm{B}^0_\mathrm{s} \to \mu^+\mu^-$, however, occurs only at one loop and so to that order there the CP-phase cancels when squaring the matrix element. The branching ratio thus only depends on modulus of the mass insertions. In what follows we shall treat the mass insertions as real, $\delta^{IJ*}_{QXY} = \delta^{IJ}_{QXY}$. The imaginary components of the mass insertions are highly constrained to be near-zero, with $|\Im\mathrm{m}(\delta^{IJ}_{QXY})|$ much less than the step size of our scan [56, 54].

The parameter space scan also incorporates the experimental constraints used in [53], which are reproduced in Figure 5.2. The results of this parameter scan are shown in Figures 5.1 and 5.2.

Quantity	Current Measurement	Experimental Error
$m_{\chi_1^0}$	> 46 GeV	
$m_{\chi_1^\pm}$	> 94 GeV	
$m_{\tilde{b}}$	> 89 GeV	
$m_{\tilde{t}}$	> 95.7 GeV	
m_h	> 92.8 GeV	
$\lvert\epsilon_K\rvert$	$2.232 \cdot 10^{-3}$	$0.007 \cdot 10^{-3}$
ΔM_d	$3.337 \cdot 10^{-13}$ GeV	$0.033 \cdot 10^{-13}$ GeV
ΔM_s	$116.96 \cdot 10^{-13}$ GeV	$0.79 \cdot 10^{-13}$ GeV
$\mathrm{Br}(B \to X_s\gamma)$	$3.34 \cdot 10^{-4}$	$0.38 \cdot 10^{-4}$
$\mathrm{Br}(K_L \to \pi^0\nu\bar{\nu})$	$< 1.5 \cdot 10^{-10}$	

Table 5.2: Constraints used throughout the MSSM scan .

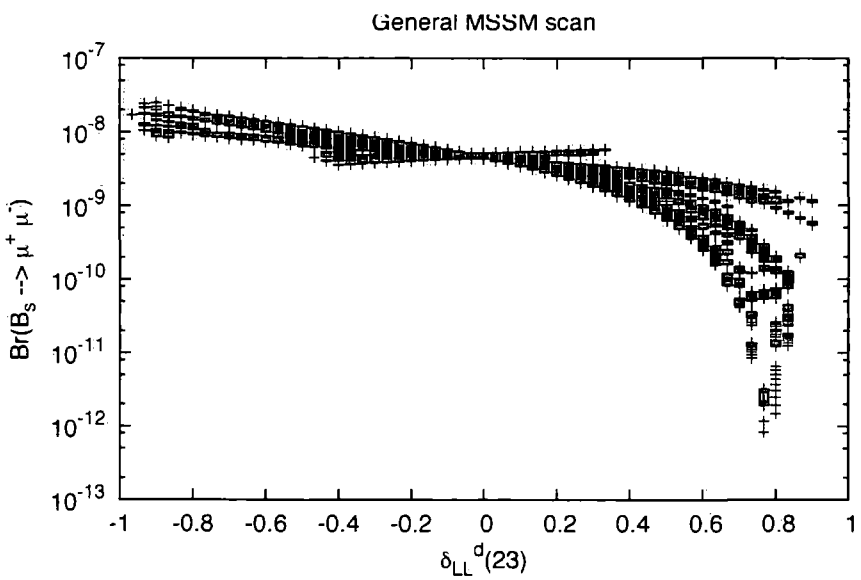

Figure 5.1: Low $\tan\beta$ MSSM prediction for $B_s^0 \to \mu^+\mu^-$ vs. LL mass insterion in the d-squark sector, δ^{23}_{dLL}.

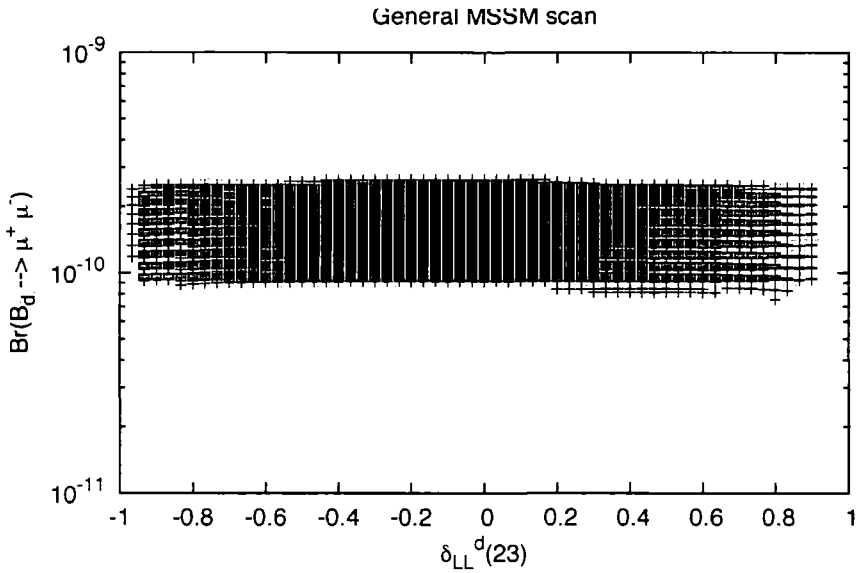

Figure 5.2: Low tan β MSSM prediction for $B_d^0 \to \mu^+ \mu^-$ vs. LL mass insterion in the d-squark sector, δ^{13}_{dLL}.

Focusing on the phenomenologically interesting $B_s^0 \to \mu^+ \mu^-$ decay channel, we can see that F_A (and hence the branching ratio) can be significantly cancelled due to the gluino-bottom squark self energy contribution in a scenario with a large mass insertion δ^{23}_{dLL}. The funnel around $\delta^{23}_{dLL} \approx 0.8$ dips below the lower bound set by our estimate of the Higgs contribution. This is notable for two reasons: (1) this is suggestive of a viable region of parameter space 'far away' from the minimal flavour violation scenario that is significantly below the Standard Model branching ratio prediction, and (2) in the regime where the Higgs contribution and the box and Z-penguins are of the same order of magnitude, it is possible that the two sets of diagrams cancel to push the branching ratio even smaller. The $B_d^0 \to \mu^+ \mu^-$ channel, on the other hand, is more stable in this region of parameter space.

References [57] and [58] bound the δ parameters for the MSSM using the mass insertion approximation (MIA) for a particular point in parameter space, $m_{\tilde{q}} = M_3 = 350$ GeV. They find that $|\delta^{23}_{dLL}| < 0.3$ and $|\delta^{23}_{dLR}| < 0.02$, seemingly ruling out the funnel region of interest. Our analysis here, however, scans over all experimentally allowed parameter space and does not resort to MIA. Still, since the Higgs contribution may be of the same order of magnitude as the Z-penguins, one must be careful to consider their effect on this funnel region. Naively, it may either push the branching ratio smaller, or possibly push it back up towards the Standard Model expectation.

Follow-up work conducted as this thesis was being completed has indeed found that the structure of minima of the branching ratios for $B_{s,d} \to \mu^+ \mu^-$ are changed upon including the Higgs penguin [1]. The minimum of $Br(B_s^0 \to \mu^+ \mu^-)$ is still on the order of 10^{-12}, but now occurs for values of δ^{23}_{dLR} on the order of 0.01. Thus there is still a non-trivial low-tan β cancellation in the dileptonic decays of the neutral B-mesons.

5.3 Outlook

Early deep sea probes surprised marine biologists with the discovery of life at depths previously believed to be uninhabitable. In the same fashion, the low tan β parameter scan for $B_s^0 \to \mu^+ \mu^-$ suggest a robust sector of MSSM theory-space far from the minimal flavour violation scenarios that have been taken as conventional dogma. A full scan incorporating the methods and results of this calculation is now underway to quantify the features of the $\delta^{23}_{dLL} \approx 0.8$ cancellation funnel in $B_s^0 \to \mu^+ \mu^-$ [1]. The results of this study, coupled with the observations of the more stable $B_d^0 \to \mu^+ \mu^-$ predictions, will be of significant importance in the event that the LHCb does not detect the $B_s^0 \to \mu^+ \mu^-$ decay mode before decisions must be made about its upgrade [12]. Given limited resources, the feasibility of measuring the $B_s^0 \to \mu^+ \mu^-$ mode with higher luminosity must be weighed against the potential gains of reaching the $B_d^0 \to \mu^+ \mu^-$ branching ratio (with perhaps more certainty).

The complete code including both this low tan β analysis and a resummed analysis for large tan β will be made availble for public use by experimentalists and phenomenologists.

We are now approaching an important time in the history of experimental particle physics. While many eyes are on the LHC general purpose detectors searching for on-shell production of new physics, it may be that nature has been kind to flavour physicists and has decided to live in a region of parameter space where an excess in the $B_s^0 \to \mu^+ \mu^-$ branching ratio can be measured immediately. As we have seen, however, nature may also be coy and choose to hide the $B_s^0 \to \mu^+ \mu^-$ mode from experimentalists. In this case, the signal for new physics in this channel would then be the *non*-signal below the Standard Model prediction. And it would then require a careful understanding of the allowed regions of parameter space to best select an experimental strategy to upgrade the LHCb to maximise future discovery potential.

Appendix A

Notation and Conventions

> *"General relativists use the metric* $-+++$*. Particle physicists use the metric* $+---$*. String theorists use the metric* $+++++++\cdots$*"*
>
> — Anonymous

We shall use the particle physics ('West Coast') $+---$ metric. Unless otherwise noted, the indices i, j, k are generally used to label flavour, though we will take the liberty to abuse this notation as a generic fermion index when the meaning is unambiguous. The indices I, J, K, L are reserved for the flavours of the external fermions in the decay $\mathrm{B}_{\mathrm{s,d}} \to \ell^+ \ell'^-$. a, b will generally label scalar particles. These index conventions are especially important in Appendix E. $P_{L,R} = \frac{1}{2}(1 \mp \gamma_5)$ are the left- and right-hand chiral projection operators. Boldfaced terms in equations are matrices in flavour space. Matrices with a hat (e.g. $\hat{m}$) are diagonal in the basis being used. Our sign and mass-diagonalisation conventions for the Standard Model follow Burgess and Moore [4], while those for the MSSM follow Rosiek [8]. In both cases we use $\xi = 1$ Feynman gauge.

Our particular naming scheme for particles may be a bit idiosyncratic, but it is motivated by what the author feels is the most natural and accessible convention. It lies somewhere between the naming conventions of Rosiek [8] and Martin [7]. Our guiding principles for this convention were that (1) physical SUSY partner particles should be indicated by tildes and (2) multiple indices should be avoided when possible. We have made an exception for the common notation of referring to the neutralinos and charginos by χ without a tilde. Otherwise, the gluinos, Higgsinos, and scalar superpartners are denoted by tildes. This is all summarised in Table 2.2. We will occasionally use a

shorthand where we write $H_a^\pm$ to label the physical charged Higgs, $H_1^\pm$, and the charged Goldstone boson that gives mass to the W, $H_2^\pm = G^\pm$. Neutralinos and charginos are indexed in order of ascending mass.

We deliberately choose to denote the two Higgs doublets with the subscripts u and d rather than 1 and 2 as is sometimes used in the literature. We find that the latter notation, while lending itself to easy indexing, is especially confusing to students since it's not clear which numbered Higgs appears in each Yukawa coupling. Further, the definition of the all-important ratio $\tan\beta$ is not manifestly clear. The author urges the community to adopt the $H_{u,d}$ notation for the sake of clarity.

Renormalisation is done in the $\overline{\text{MS}}$ scheme with dimensional regularisation. We will use the conventional notation and write the renormalisation scale as μ with the assumption that context will prevent ambiguities with the muon. The relevant 'Buras' conventions for loop integrals are given in Appendix D, these closely follow Axelrod [59] up to the sign of the first argument of the B_1 function.

Finally, we attempt to consistently use British English spellings and conventions. The author apologises for any Yankee mistakes.

Appendix B

Diagonalisation of MSSM masses

"So how do you diagonalise a quadratic form? This reminds me of a saying in the USSR. What do you do if there's a nuclear attack? Well, you cover your head and slowly walk to the cemetary."

— Y. Eliashberg, to confused first year mathematics students

In this section we define the mixing matrices involved in diagonalising the MSSM physical spectrum. We reproduce Section 4 of [8] using this work's notation and conventions and inserting our own commentary where appropriate.

B.1 Electroweak symmetry breaking

Upon electroweak symmetry breaking, the up- and down-type Higgses receive vacuum expectation values (vevs)

$$\langle H_u \rangle = \frac{1}{\sqrt{2}} \begin{pmatrix} 0 \\ v_u \end{pmatrix} \qquad \langle H_d \rangle = \frac{1}{\sqrt{2}} \begin{pmatrix} v_d \\ 0 \end{pmatrix}. \tag{B.1}$$

The ratio of the two vevs is defined to be $\tan\beta = v_u/v_d$. The vevs are constrained to reproduce the correct gauge boson masses, i.e. $v_u^2 + v_d^2 = v_{\mathrm{SM}}^2$. Further self-consistency

among the MSSM parameters require

$$\left[\frac{e^2}{8s_W^2c_W^2}\left(v_u^2+v_d^2\right)+m_{H_d}^2+|\mu|^2\right]v_d = -m_{12}^2v_u \tag{B.2}$$

$$\left[\frac{e^2}{8s_W^2c_W^2}\left(v_u^2-v_d^2\right)+m_{H_u}^2+|\mu|^2\right]v_u = -m_{12}^2v_d. \tag{B.3}$$

We have written s_W and c_W for $\sin\theta_W$ and $\cos\theta_W$ respectively. θ_W is the Weinberg angle.

B.2 Gauge bosons

The eight gluons g^a and the photon γ are massless, while the $W^\pm$ and Z have masses

$$M_Z = \frac{e}{2s_Wc_W}\sqrt{v_u^2+v_d^2} \tag{B.4}$$

$$M_W = \frac{e}{2s_W}\sqrt{v_u^2+v_d^2} \tag{B.5}$$

B.3 Charged scalar Higgses

Of the four charged scalar Higgses, two have masses

$$M_{H_1^\pm} = M_W^2+m_{H_d}^2+m_{H_u}^2+2|\mu|^2. \tag{B.6}$$

The other two charged scalar Higgses become the Goldstone bosons that are 'eaten' by the $W\pm$-boson. The $H_{1,2}^\pm$ fields are related to the initial $H_{u,d}$ fields by the rotation matrix Z_H:

$$\begin{pmatrix} H_u^{1*} \\ H_d^2 \end{pmatrix} = Z_H \begin{pmatrix} H_1^+ \\ H_2^+ \end{pmatrix}, \tag{B.7}$$

(B.8)

which is explicitly given in terms of the Higgs vevs as

$$Z_H = \frac{1}{\sqrt{v_u^2+v_d^2}}\begin{pmatrix} v_u & -v_d \\ v_d & v_u \end{pmatrix}. \tag{B.9}$$

B.4 Neutral scalar Higgses

The neutral Higgses are divided into the $\mathcal{CP}$-even Higgses h, H and the $\mathcal{CP}$-odd Higgs A^0. A fourth $\mathcal{CP}$-odd Higgs is the Goldstone boson that is 'eaten' by the Z-boson. The $\mathcal{CP}$ terminology only strictly holds if the Lagrangian contains only real parameters in the Higgs sector, though the classification of the particles in this limit is standard even if the Lagrangian contains complex parameters.

The 'scalar' Higgses H_i^0 ($H_1^0 = h$ and $H_2^0 = H$) are defined as

$$\sqrt{2}\mathrm{Re}H_d^1 = Z_R^{1i} H_i^0 + v_d \tag{B.10}$$

$$\sqrt{2}\mathrm{Re}H_u^2 = Z_R^{2i} H_i^0 + v_u. \tag{B.11}$$

Meanwhile, the 'pseudoscalar' Higgses A_i^0 ($A_1^0 = A^0$ and $A_2^0 = G^0$, the Goldstone boson) are defined as

$$\sqrt{2}\mathrm{Im}H_d^1 = Z_H^{1i} A_i^0 \tag{B.12}$$

$$\sqrt{2}\mathrm{Im}H_u^2 = Z_H^{2i} A_i^0. \tag{B.13}$$

The mass of the $\mathcal{CP}$-odd Higgs is

$$M_{A^0}^2 = m_{H_u}^2 + m_{H_d}^2 + 2|\mu|^2. \tag{B.14}$$

The Z_H mixing matrix is precisely the same as that for the neutral scalar Higgses. Meanwhile, the Z_R matrix is given by

$$Z_R = \begin{pmatrix} \cos\alpha & -\sin\alpha \\ \sin\alpha & \cos\alpha \end{pmatrix}, \tag{B.15}$$

$$\tan 2\alpha = \tan 2\beta \frac{M_A^2 + M_Z^2}{M_A^2 - M_Z^2}. \tag{B.16}$$

B.5 Standard Model fermions

The Standard Model fermions are defined as usual with masses coming from the Yukawa couplings after electroweak symmetry breaking.

$$m_\nu^i = 0 \qquad m_e^i = -\frac{v_d y_\ell^i}{\sqrt{2}} \tag{B.17}$$

$$m_d^i = -\frac{v_d y_d^i}{\sqrt{2}} \qquad m_u^i = \frac{v_u y_u^i}{\sqrt{2}} \tag{B.18}$$

In this convention note that the H_d Yukawa couplings are defined to be negative.

B.6 Charginos

The Majorana spinors $\tilde{A}^1$ and $\tilde{A}^2$ combine with the Weyl spinors $\tilde{H}_u^1$ and $\tilde{H}_d^2$ to form the two chargino Dirac spinors $\chi_{1,2}$. The mixing in $(\tilde{A}^1, \tilde{A}^2, \tilde{H}_u^1, \tilde{H}_d^2)$ space is given by the singular value decomposition

$$(Z_-)^T \begin{pmatrix} M_2 & \frac{ev_2}{\sqrt{2}s_W} \\ \frac{ev_1}{\sqrt{2}s_W} & \mu \end{pmatrix} Z_+ = \begin{pmatrix} M_{\chi_1} & 0 \\ 0 & M_{\chi_2} \end{pmatrix}. \tag{B.19}$$

The unitary matrices Z_+ and Z_- are not uniquely specified. We choose their phases such that $M_{\chi_2} > M_{\chi_1}$. The fields χ_i are related to the initial spinors via:

$$\tilde{H}_d^2 = Z_+^{2i} \kappa_i^+ \tag{B.20}$$

$$\tilde{H}_u^1 = Z_-^{2i} \kappa_i^- \kappa_i^+ \tag{B.21}$$

$$\frac{\tilde{A}^1 \mp i\tilde{A}^2}{\sqrt{2}} = i Z_\pm^{1i} \kappa_i^\pm \tag{B.22}$$

$$\chi_i = \begin{pmatrix} \kappa_i^+ \\ \overline{\kappa_i^-} \end{pmatrix} \tag{B.23}$$

B.7 Neutralinos

The Majorana spinors $\tilde{B}$ and $\tilde{A}^3$ combine with the Weyl spinors $\tilde{H}_d^1$ and $\tilde{H}_u^2$ to form the four Neutralino Majorana spinors $\chi^0_{1,\cdots,4}$. The mixing in $(\tilde{B}, \tilde{A}^4, \tilde{H}_d^1, \tilde{H}_u^2)$ space is given

by the Takagi factorisation [60]

$$Z_N^T \begin{pmatrix} M_1 & 0 & \frac{-ev_d}{2c_W} & \frac{ev_u}{2c_W} \\ 0 & M_2 & \frac{ev_d}{2s_W} & \frac{-ev_u}{2s_W} \\ \frac{-ev_d}{2c_W} & \frac{ev_d}{2s_W} & 0 & -\mu \\ \frac{ev_u}{2c_W} & \frac{-ev_u}{2s_W} & -\mu & 0 \end{pmatrix} Z_N = \begin{pmatrix} M_{\chi_1^0} & & 0 \\ & \ddots & \\ 0 & & M_{\chi_4^0} \end{pmatrix}. \tag{B.24}$$

The fields χ_i^0 are related to the initial spinors via:

$$\lambda_B = iZ_N^{1i}\kappa_i^0 \tag{B.25}$$

$$\lambda_A^3 = iZ_N^{2i}\kappa_i^0 \tag{B.26}$$

$$\Psi_{H1}^1 = Z_N^{3i}\kappa_i^0 \tag{B.27}$$

$$\Psi_{H2}^2 = Z_N^{4i}\kappa_i^0 \tag{B.28}$$

$$\chi_i^0 = \begin{pmatrix} \kappa_i^0 \\ \overline{\kappa}_i^0 \end{pmatrix}. \tag{B.29}$$

B.8 Gluinos

The eight Majorana spinor gluinos $\tilde{g}^a$ do not mix.

B.9 Sneutrinos

The complex scalar fields $\tilde{\nu}_L^i$ form (neutral) complex scalar sneutrino eigenstates $\tilde{\nu}^i$. The mixing is given by

$$Z_\nu^\dagger \mathcal{M}_\nu^2 Z_\nu = \begin{pmatrix} M_{\nu_1}^2 & & 0 \\ & \ddots & \\ 0 & & M_{\nu_3}^2 \end{pmatrix} \tag{B.30}$$

$$\mathcal{M}_\nu^2 = \frac{e^2(v_1^2 - v_2^2)}{8s_W^2 c_W^2}\hat{1} + m_L^2, \tag{B.31}$$

where the fields $\tilde{\nu}^i$ are related to the initial scalars via $\tilde{\nu}_L^i = Z_\nu^{ij}\tilde{\nu}^j$.

B.10 Selectrons

The complex scalar fields $\tilde{e}^i_L$ and $\tilde{e}^i_R$ $(i = 1, \cdots, 3)$ mix to give six charged selectrons $\tilde{e}^i$, $(i = 1, \cdots, 6)$:

$$Z_L^\dagger \begin{pmatrix} (\mathcal{M}_L^2)_{LL} & (\mathcal{M}_L^2)_{LR} \\ (\mathcal{M}_L^2)^\dagger_{LR} & (\mathcal{M}_L^2)_{RR} \end{pmatrix} Z_L = \begin{pmatrix} M^2_{L_1} & & 0 \\ & \ddots & \\ 0 & & M^2_{L_6} \end{pmatrix} \tag{B.32}$$

$$(\mathcal{M}_L^2)_{LL} = \frac{e^2(v_d^2 - v_u^2)(1 - 2c_W^2)}{8 s_W^2 c_W^2} \mathbb{I} + \frac{v_d^2 \mathbf{y_\ell^2}}{2} + (\mathbf{m_L}^2)^T \tag{B.33}$$

$$(\mathcal{M}_L^2)_{RR} = -\frac{e^2(v_d^2 - v_u^2)}{4c_W^2} \mathbb{I} + \frac{v_d^2 \mathbf{y_\ell^2}}{2} + \mathbf{m_R}^2 \tag{B.34}$$

$$(\mathcal{M}_L^2)_{LR} = \frac{1}{\sqrt{2}} \left(v_d (\mathbf{y}_\ell \mu^* - \mathbf{a}'_\ell) + v_d \mathbf{a}_\ell \right). \tag{B.35}$$

The fields $\tilde{e}^i$ are related to the initial fields via

$$\tilde{e}^i_L = Z_L^{ij*} \tilde{e}^j \qquad \tilde{e}^i_R = Z_L^{(i+3)j} \tilde{e}^j. \tag{B.36}$$

B.11 Up squarks

The complex scalar fields $\tilde{u}^i_L$ and $\tilde{u}^i_R (i = 1, \cdots, 3)$ mix to give six up squarks $\tilde{u}^i$, $(i = 1, \cdots, 6)$:

$$Z_U^T \begin{pmatrix} (\mathcal{M}_U^2)_{LL} & (\mathcal{M}_U^2)_{LR} \\ (\mathcal{M}_U^2)^\dagger_{LR} & (\mathcal{M}_U^2)_{RR} \end{pmatrix} Z_U^\star = \begin{pmatrix} M^2_{U_1} & & 0 \\ & \ddots & \\ 0 & & M^2_{U_6} \end{pmatrix} \tag{B.37}$$

$$(\mathcal{M}_U^2)_{LL} = -\frac{e^2(v_d^2 - v_u^2)(1 - 4c_W^2)}{24 s_W^2 c_W^2}\mathbb{I} + \frac{v_d^2 \mathbf{y_u}^2}{2} + (\mathbf{V m_Q^2 V^\dagger})^T \quad \text{(B.38)}$$

$$(\mathcal{M}_U^2)_{RR} = \frac{e^2(v_d^2 - v_u^2)}{6c_W^2}\mathbb{I} + \frac{v_d^2 \mathbf{y_u}^2}{2} + \mathbf{m_U}^2 \quad \text{(B.39)}$$

$$(\mathcal{M}_U^2)_{LR} = -\frac{1}{\sqrt{2}}\left(v_d(\mathbf{a_u'} + \mathbf{y_u}\mu^*) + v_u \mathbf{a_u}\right). \quad \text{(B.40)}$$

The fields $\tilde{u}^i$ are related to the initial fields via

$$\tilde{u}_L^i = Z_U^{ij}\tilde{u}^j \qquad \tilde{u}_R^i = Z_U^{(i+3)j*}\tilde{u}^j. \quad \text{(B.41)}$$

B.12 Down squarks

The complex scalar fields $\tilde{d}_L^i$ and $\tilde{d}_R^i (i = 1, \cdots, 3)$ mix to give six up squarks $\tilde{d}^i$, $(i = 1, \cdots, 6)$:

$$Z_D^\dagger \begin{pmatrix} (\mathcal{M}_D^2)_{LL} & (\mathcal{M}_D^2)_{LR} \\ (\mathcal{M}_D^2)_{LR}^\dagger & (\mathcal{M}_D^2)_{RR} \end{pmatrix} Z_D = \begin{pmatrix} M_{D_1}^2 & & 0 \\ & \ddots & \\ 0 & & M_{D_6}^2 \end{pmatrix} \quad \text{(B.42)}$$

$$(\mathcal{M}_D^2)_{LL} = -\frac{e^2(v_d^2 - v_u^2)(1 + 2c_W^2)}{24 s_W^2 c_W^2}\mathbb{I} + \frac{v_d^2 \mathbf{y_d}^2}{2} + (\mathbf{m_Q}^2)^T \quad \text{(B.43)}$$

$$(\mathcal{M}_D^2)_{RR} = -\frac{e^2(v_d^2 - v_u^2)}{12c_W^2}\mathbb{I} + \frac{v_d^2 \mathbf{y_d}^2}{2} + \mathbf{m_D}^2 \quad \text{(B.44)}$$

$$(\mathcal{M}_D^2)_{LR} = \frac{1}{\sqrt{2}}\left(v_u(\mathbf{y_d}\mu^* - \mathbf{a_d'}) + v_d \mathbf{a_d}\right). \quad \text{(B.45)}$$

The fields $\tilde{d}^i$ are related to the initial fields via

$$\tilde{d}_L^i = Z_D^{ij*}\tilde{d}^j \qquad \tilde{d}_R^i = Z_D^{(i+3)j}\tilde{d}^i. \quad \text{(B.46)}$$

Appendix C

Fierz Identities

"Some of the most important results are so surprising at first sight that nothing short of a proof can make them credible."

— Sir Harold Jeffreys, *Methods of Mathematical Physics*

Here we collect a list of Fierz identities, with and without the charge conjugation matrix C. Those with charge conjugation matrices are relevant for calculations with Majorana fermions. Here i, j, k, ℓ label spinor indices. Note that we do not include factors of (-1) from fermion anticommutation. Further details about deriving these rules can be found in Nishi [61] and Nieves and Pal [62].

C.1 Fierz identities without a C-matrix

$$(\gamma^\mu P_{L,R})_{ij}(\gamma_\mu P_{L,R})_{k\ell} = -(\gamma^\mu P_{L,R})_{i\ell}(\gamma_\mu P_{L,R})_{kj} \quad \text{(C.1)}$$

$$(\gamma^\mu P_{L,R})_{ij}(\gamma_\mu P_{R,L})_{k\ell} = 2(P_{R,L})_{i\ell}(P_{L,R})_{kj} \quad \text{(C.2)}$$

$$(P_{L,R})_{ij}(P_{L,R})_{k\ell} = \frac{1}{2}(P_{L,R})_{i\ell}(P_{L,R})_{kj} + \frac{1}{8}(\sigma^{\mu\nu})_{i\ell}(\sigma_{\mu\nu}P_{L,R})_{kj} \quad \text{(C.3)}$$

$$(P_{L,R})_{ij}(P_{R,L})_{k\ell} = \frac{1}{2}(\gamma^\mu P_{R,L})_{i\ell}(\gamma_\mu P_{L,R})_{kj} \quad \text{(C.4)}$$

$$(\sigma^{\mu\nu})_{ij}(\sigma_{\mu\nu}P_{L,R})_{k\ell} = 6(P_{R,L})_{i\ell}(P_{L,R})_{kj} - \frac{1}{2}(\sigma^{\mu\nu})_{i\ell}(\sigma_{\mu\nu}P_{L,R})_{kj} \quad \text{(C.5)}$$

$$(\sigma^{\mu\nu})_{i\ell}(\sigma_{\mu\nu}P_{L,R})_{kj} = \frac{1}{2}(g^{\mu\alpha}g^{\nu\beta} \mp \frac{1}{2}i\epsilon^{\mu\nu\alpha\beta})(\sigma_{\mu\nu})_{i\ell}(\sigma_{\alpha\beta})_{kj} \quad \text{(C.6)}$$

C.2 Fierz identities with a C-matrix

$$(\gamma^\mu P_{L,R}C)_{ij}(C\gamma_\mu P_{L,R})_{k\ell} = -2(P_{R,L})_{ik}(P_{L,R})_{j\ell} \quad \text{(C.7)}$$

$$(\gamma^\mu P_{L,R}C)_{ij}(C\gamma_\mu P_{R,L})_{k\ell} = -(\gamma^\mu P_{L,R})_{ik}(\gamma_\mu P_{R,L})_{j\ell} \quad \text{(C.8)}$$

$$(P_{L,R}C)_{ij}(CP_{L,R})_{k\ell} = \frac{1}{2}(P_{L,R})_{ik}(P_{L,R})_{j\ell} - \frac{1}{8}(\sigma^{\mu\nu})_{ik}(\sigma_{\mu\nu}P_{L,R})_{j\ell} \quad \text{(C.9)}$$

$$(P_{L,R}C)_{ij}(CP_{R,L})_{k\ell} = -\frac{1}{2}(\gamma^\mu P_{R,L})_{ik}(\gamma_\mu P_{R,L})_{j\ell} \quad \text{(C.10)}$$

Appendix D

Loop Integrals

"Pi is almost dimensionful. $4\pi^2$ has dimensions of inverse loop."
— S. Dimopoulos

Since much of the focus in B physics is on loop-level effects, it is important to have a collection of loop integrals available. Most quantum field theory textbooks would present the standard pedagogical canon for performing such integrals using the technique of Feynman parameters. Unfortunately, this technique becomes overly cumbersome for even moderately complicated integrals. For many diagrams, such as the boxes and the 1PI penguins, the smallness of external state masses relative to the masses of loop particles allows us to take the limit where the external particles are massless. These integrals are particularly easy to solve using algebraic recursion relations. Since these recursion relations aren't usually taught to students, we present them pedagogically in Section D.1.

Next, in Section D.2, we cite all the result of the relevant loop integrals for this work for easy reference. In particular, the Passarino-Veltman B functions appear in the self-energy penguin diagrams and are a bit more difficult to derive as they require one to maintain nonzero external momenta. Detailed discussions on the 'art' of doing loop integrals are available in Pokorski's text [63], the original paper by Passarino and Veltman [64], Weinzierl's notes [65], or the Compendium of Relations 2.1 [66].

D.1 Algebraic techniques for simple loop integrals

It is important for young physicists to learn how to separate 'physics' from 'mathematics.' As a rule of thumb, 'physics' is usually dimensionful and is often interesting for how certain quantities scale with respect to other quantities. 'Mathematics,' on the other hand, can be written in terms of functions of dimensionless variables (ratios) that can be plugged into a computer for analytic or numeric values. In the case of loop-level diagrams, this separation means disentangling various masses and momenta so that one is left with a generic loop integral that can be looked up in a table. Here we shall demonstrate simple methods for performing such integrals in the limiting case where external momenta can be ignored.

Before starting, factor out all couplings and overall constants outside of the integral. One must then completely remove the nontrivial Dirac structure of the amplitude by taking the appropriate traces of γ-matrices. Fermion propagators then leave products of numerators of the form

$$k_{\mu_1} k_{\mu_2} \cdots k_{\mu_n}.$$

These are contracted against factors of the metric which came about from simplifying the γ-matrices. Note that the assumption that the external momenta vanish means that the denominator of the integral takes the form

$$(k^2 - m_1^2)(k^2 - m_2^2) \cdots (k^2 - m_p^2).$$

The important feature here is that the denominator of the integral is spherically symmetric. Hence the entire integral vanishes by symmetry if the power of k_μ in the numerator is odd. For even powers of k_μ, we can use the fact that a symmetric product of vectors is equal to a linear combination of products of the metric. Thus:

$$k_{\mu_1} \cdots k_{\mu_{2n}} \quad \propto \quad k^{2n} \sum_i g_{\mu_{i_1}\mu_{i_2}} \cdots g_{\mu_{i_{2n-1}}\mu_{i_{2n}}}. \tag{D.1}$$

The overall coefficient can be worked out by contracting both sides with, for example, $g_{\mu_1\mu_2} \cdots g_{\mu_{2n-1}\mu_{2n}}$. While this becomes tedious for $n > 3$, one can work out the first three coefficients in general spacetime dimension to find a nice pattern.

After this quick analysis, one is left with a sum of integrals of the form

$$I_p^{(2n)}(m_1, \cdots, m_p) = \int \frac{d^4k}{(2\pi)^4} \frac{k^{2n}}{(k^2 - m_1^2)(k^2 - m_2^2) \cdots (k^2 - m_p^2)}. \quad \text{(D.2)}$$

Such an integral is tedious for medium and large values of n and p. Our strategy will be to reduce this into a sum of integrals with smaller values of n and p. It turns out that this is very simple to do with the following algebraic relations:

$$\frac{k^2}{k^2 - m^2} = 1 + \frac{m^2}{k^2 - m^2} \quad \text{(D.3)}$$

$$\frac{1}{(k^2 - m_1^2)(k^2 - m_1^2)} = \frac{1}{m_1^2 - m_2^2}\left(\frac{1}{k^2 - m_1^2} - \frac{1}{k^2 - m_2^2}\right). \quad \text{(D.4)}$$

Voilà! Equation (D.3) reduces the power of the numerator by two, taking an integral of the form $I_p^{(2n)}$ into a sum of integrals of the form $I_{p-1}^{(2n-2)}$ and $I_p^{(2n-2)}$. Similarly, equation (D.4) reduces the power of the denominator by one, taking an integral of the form $I_p^{(2n)}$ into a difference of integrals of the form $I_{p-1}^{(2n)}$. The resulting reduction rules, written out explicitly, are:

$$I_p^{(2n)}(m_1^2, \cdots, m_p^2) = I_{p-1}^{(2n-2)}(m_1^2, \cdots, m_{p-1}^2) + m_p^2 I_p^{(2n-2)}(m_1^2, \cdots, m_{p-1}^2) \quad \text{(D.5)}$$

$$I_p^{(2n)}(m_1^2, \cdots, m_p^2) = \frac{1}{m_1^2 - m_p^2}\left[I_{p-1}^{(2n)}(m_1^2, \cdots, m_{p-1}^2) - I_{p-1}^{(2n)}(m_2^2, \cdots, m_p^2)\right]. \quad \text{(D.6)}$$

The number of terms, of course, grows by a factor of two every time these reductions are applied, but one can continue this trick until all terms are written in terms of two simple functions: the divergent $I_2^{(0)}$ and the convergent $I_3^{(0)}$. These can then be solved explicitly using one's preferred method. The results using our conventions, Wick rotation, and dimensional regularisation in $4 - \epsilon$ dimensions are:

$$I_2^{(0)}(m_1^2, m_2^2) = \frac{i}{(4\pi)^2}\left[\frac{2}{\epsilon} - \gamma_E + \log\left(\frac{4\pi}{m_1^2}\right) + 1 + \frac{x}{1-x}\log x\right] \quad \text{(D.7)}$$

$$I_2^{(0)}(m_1^2, m_2^2, m_3^2) = \frac{1}{m_1^2(x-y)}\frac{i}{(4\pi)^2}\left[\frac{x}{1-x}\log x - \frac{y}{1-y}\log y\right], \quad \text{(D.8)}$$

where we write $x = m_2^2/m_1^2$ and $y = m_3^2/m_1^2$. Note that though the above equations aren't manifestly equivalent under interchange of the arguments due to this choice of x and y, explicit calculation will show that one may reshuffle the order of the arguments without changing the result.

Finally, we note that the algebraic tricks above fail if two of the masses are equivalent. In this case, however, one can still use the tricks with all pairwise inequivalent masses to reduce the integral to the form $I_q^{(2k)}(m^2, \cdots, m^2)$. This is a particularly well-known integral that can be performed using the Γ function:

$$\int \frac{d^n k}{(2\pi)^n} \frac{(k^2)^b}{(k^2 - A^2)^a} = \frac{i}{(4\pi)^{n/2}} (-1)^{a+b} \left(A^2\right)^{b-a+n/2} \frac{\Gamma(b + n/2)\Gamma(a - b - n/2)}{\Gamma(n/2)\Gamma(a)},$$

where we note that the left-hand side is an integral in n-dimensional Minkowski space.

D.2 Useful loop integral results

Here we collect the analytic forms of the relevant loop integrals for this work. We follow the 'Buras' convention of Appendix A.5 in [36]. This convention matches the popular convention of Axelrod [59] up to the sign of the first argument of the B_1 function.

The two-point loop integral B_1 is defined as:

$$\frac{1}{(4\pi)^2} p_\mu B_1(p, m^2, M^2) = \int \frac{d^d k}{(2\pi)^2} \frac{i k_\mu}{(k^2 - m^2)\left[(k + p)^2 - M^2\right]}. \tag{D.9}$$

These integrals appear in the flavour-changing quark self-energy contributions to the penguin diagrams. It is necessary to keep the external momentum p_μ general (i.e. nonzero) until it can be converted into an external mass in the amplitude, after which point one may take $B_1(p, m^2, M^2) \to B_1(0, m^2, M^2)$.

The three- and four-point loop integrals at vanishing external momenta are defined as:

$$\frac{1}{(4\pi)^2} C_{2n}(m_1^2, m_2^2, m_3^2) = \int \frac{d^d k}{(2\pi)^2} \frac{i k^{2n}}{\prod_i^3 (k^2 - m_i^2)} \tag{D.10}$$

$$\frac{1}{(4\pi)^2} D_{2n}(m_1^2, m_2^2, m_3^2, m_4^2) = \int \frac{d^d k}{(2\pi)^2} \frac{i k^{2n}}{\prod_i^4 (k^2 - m_i^2)}. \tag{D.11}$$

The explicit formula for the two-point loop integral B_1 at vanishing external momentum is:

$$B_1(0, x, y) = \frac{1}{4} + \frac{1}{2} C_2(x, y, y), \tag{D.12}$$

where $C_2(x,y,y)$ is given below.

The explicit formulae for the three-point integrals at vanishing external momenta are:

$$C_0(x,y,z) = \frac{y\log\frac{y}{x}}{(x-y)(z-y)} + \frac{z\log\frac{z}{x}}{(x-z)(y-z)} \tag{D.13}$$

$$C_0(x,y,y) = \frac{1}{x-y}\left[1 - \frac{x\log\frac{x}{y}}{x-y}\right] \tag{D.14}$$

$$C_2(x,y,z) = \Delta + \log\frac{\mu^2}{x} + \frac{y^2\log\frac{y}{x}}{(x-y)(z-y)} + \frac{z^2\log\frac{z}{x}}{(x-z)(y-z)} \tag{D.15}$$

$$C_2(x,y,y) = \Delta + \log\frac{\mu^2}{y} + \frac{x}{x-y}\left[1 - \frac{x\log\frac{x}{y}}{x-y}\right], \tag{D.16}$$

where the divergent piece $\Delta = \frac{2}{d-4} + \log(4\pi)\gamma_E - 1$ and μ is the renormalisation scale. These integrals appear in the Z-penguin contributions.

The explicit formulae for the four-point integrals at vanishing external momenta are:

$$D_0(x,y,z,t) = \frac{y\log\frac{y}{x}}{(y-x)(y-z)(y-t)} + \frac{z\log\frac{z}{x}}{(z-x)(z-y)(z-t)} + \frac{t\log\frac{t}{x}}{(t-x)(t-y)(t-z)} \tag{D.17}$$

$$D_0(x,y,z,z) = -\frac{1}{(x-z)(y-z)} - \frac{x\log\frac{x}{z}}{(x-y)(x-z)^2} - \frac{y\log\frac{y}{z}}{(y-x)(y-z)^2} \tag{D.18}$$

$$D_2(x,y,z,t) = \frac{y^2\log\frac{y}{x}}{(y-x)(y-z)(y-t)} + \frac{z^2\log\frac{z}{x}}{(z-x)(z-y)(z-t)} + \frac{t^2\log\frac{t}{x}}{(t-x)(t-y)(t-z)} \tag{D.19}$$

$$D_2(0,x,y,z) = \frac{1}{y-z}\left(\frac{x\log\frac{x}{z}}{x-z} - \frac{y\log\frac{y}{z}}{y-z}\right) \tag{D.20}$$

$$D_2(0,x,x,y) = \frac{1}{y-x}\left(1 - \frac{y\log\frac{y}{x}}{y-x}\right) \tag{D.21}$$

$$D_2(x,y,z,z) = -\frac{z}{(x-z)(y-z)} - \frac{x^2\log\frac{x}{z}}{(x-y)(x-z)^2} - \frac{y^2\log\frac{y}{z}}{(y-x)(y-z)^2}. \tag{D.22}$$

$$\tag{D.23}$$

These integrals appear in the box diagram contributions. A null argument represents the negligible mass of the neutrino.

Appendix E

Wilson coefficients

"A chef does not need to know gauge theory."
— S. Dimopoulos, summarising the renormalisation group

Here we collect the explicit forms of the box and Z-penguin contributions to the Wilson coefficients in terms of generic Feynman rules. The effective Hamiltonian is given by equation (4.4). In the following sections we list contributions to each Wilson coefficient $\left(C^Z_{XY}\right)_i$, where i labels the contribution from a particular diagram. The full coefficient is given by the sum of each contribution, $C^Z_{XY} = \sum_i \left(C^Z_{XY}\right)_i$. Explicit diagrams for all the processes in this appendix are shown in Section 4.6.

E.1 Feynman Rules

We use a shorthand and write generic Feynman rules for the calculations below. Values for the generic couplings can be inserted from [67]. We denote the left- and right-handed spinor projectors by $P_{L,R} = \frac{1}{2}(1 \mp \gamma^5)$. S_a and f^j are generic scalars and fermions, respectively. In order to avoid clutter, we suppress particle names in the effective couplings, i.e. we write S^{ija}_L to mean $S^{ija}_{dfs,L}$.

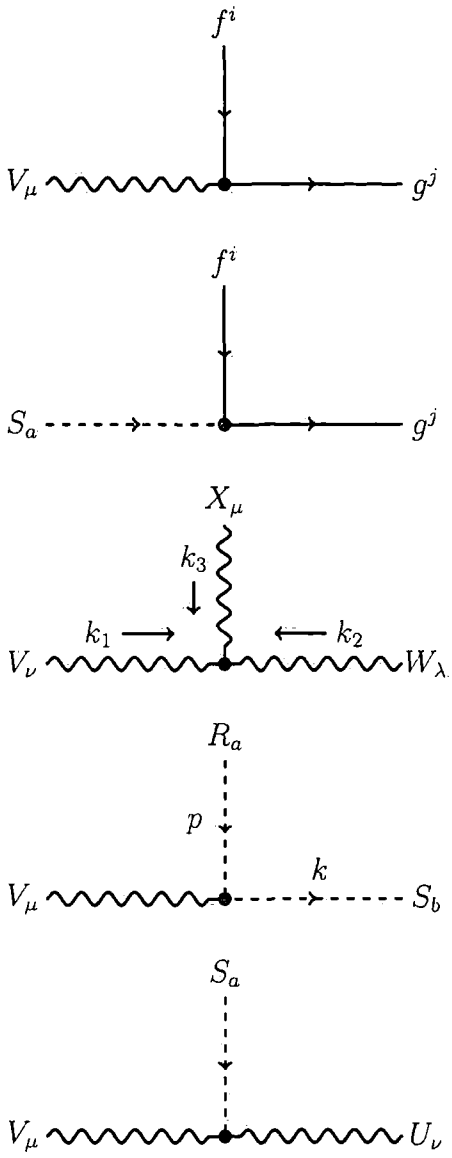

$$= iV_{fgV}^{Lij}\,\gamma_\mu P_L$$

$$= i\left(V_{fgS}^{Lija}\,P_L + V_{fgS}^{Rija}\,P_R\right)$$

$$= iV_{VWX}\left(g^{\nu\lambda}(k_1-k_2)^\mu + g^{\lambda\mu}(k_2-k_3)^\nu + g^{\mu\nu}(k_3-k_1)^\lambda\right)$$

$$= iV_{RSV}^{ab}\,(p+k)^\mu$$

$$= iV_{SVU}^{a}g^{\mu\nu}$$

E.1.1 Box Diagram Contribution

Box contributions to the Wilson coefficients are written here in the form $\left(C_{XY}^{Z\square}\right)_i$, with the $\square$ denoting box-diagram contribution. Z labels the operator, $Z = S, V, T$ for scalar, vector, tensor respectively. XY labels the handedness, $X, Y \in \{L, R\}$ with $\bar{X} = R$ if $X = L$ and vice versa. i labels the particular diagrams included in the term.

W/Goldstone contributions

$$
\begin{aligned}
\left(C_{LL}^{V\Box}\right)_W &= \sum_{i,j=1}^{3} V_{duW}^{LJi*} V_{duW}^{LIi} V_{\ell\nu W}^{L\ell j*} V_{\ell\nu W}^{LKj} \quad D_2(m_{u_i}^2, m_{\nu_j}^2, M_W^2, M_W^2) \\
&\quad - \sum_{i,j=1}^{3} \sum_{a=1}^{2} V_{duH}^{LJia*} V_{duW}^{LIi} V_{\ell\nu W}^{L\ell j*} V_{\ell\nu H}^{LKja} m_{u_i} m_{u_j} \quad D_0(m_{u_i}^2, m_{\nu_j}^2, m_{H_a}^2, M_W^2) \\
&\quad - \sum_{i,j=1}^{3} \sum_{a=1}^{2} V_{duW}^{LJi*} V_{duH}^{LIia} V_{\ell\nu H}^{L\ell ja*} V_{\ell\nu W}^{LKj} m_{u_i} m_{u_j} \quad D_0(m_{u_i}^2, m_{\nu_j}^2, m_{H_a}^2, M_W^2) \\
\left(C_{LR}^{S\Box}\right)_W &= - \sum_{i,j=1}^{3} \sum_{a=1}^{2} V_{duH}^{RJia*} V_{duW}^{LIi} V_{\ell\nu W}^{L\ell j*} V_{\ell\nu H}^{RKja} \quad D_2(m_{u_i}^2, m_{\nu_j}^2, m_{H_a}^2, M_W^2) \\
\left(C_{RL}^{S\Box}\right)_W &= - \sum_{i,j=1}^{3} \sum_{a=1}^{2} V_{duW}^{LJi*} V_{duH}^{RIia} V_{\ell\nu H}^{R\ell ja*} V_{\ell\nu W}^{LKj} \quad D_2(m_{u_i}^2, m_{\nu_j}^2, m_{H_a}^2, M_W^2)
\end{aligned}
$$

Pure Higgs/Goldstone contributions

$X, Y \in \{L, R\}$ refer to helicities, while bars refer to the opposite helicity. For example, $\bar{X} = L$ if $X = R$.

$$
\begin{aligned}
\left(C_{XY}^{V\Box}\right)_h &= \frac{1}{4} \sum_{i,j=1}^{3} \sum_{a,b=1}^{2} V_{duH}^{XJia*} V_{duH}^{XIib} V_{\ell\nu H}^{Y\ell jb*} V_{\ell\nu H}^{YKja} \quad D_2(m_{u_i}^2, m_{u_j}^2, m_{H_a}^2, m_{H_b}^2) \\
\left(C_{XY}^{S\Box}\right)_h &= \sum_{i,j=1}^{3} \sum_{a,b=1}^{2} V_{duH}^{\overline{X}Jia*} V_{duH}^{XIib} V_{\ell\nu H}^{\overline{Y}\ell jb} V_{\ell\nu H}^{YKja} m_{u_i} m_{u_j} \quad D_0(m_{u_i}^2, m_{u_j}^2, m_{H_a}^2, m_{H_b}^2)
\end{aligned}
$$

Neutralino contributions

$$
\begin{aligned}
\left(C_{LL}^{V\Box}\right)_{\chi^0} &= \frac{1}{2}\sum_{i,j=1}^{4}\sum_{a,b=3}^{2} V_{dD\chi^0}^{LJia*} V_{dD\chi^0}^{LIja} V_{\ell E\chi^0}^{L\ell ib*} V_{\ell E\chi^0}^{LKjb} m_{\chi_i^0} m_{\chi_j^0} \quad D_0(m^2_{\chi_i^0}, m^2_{\chi_j^0}, m^2_{U_a}, m^2_{E_b}) \\
&\quad + \frac{1}{4}\sum_{i,j=1}^{4}\sum_{a,b=1}^{3} V_{dD\chi^0}^{LJia*} V_{dD\chi^0}^{LIja} V_{\ell E\chi^0}^{L\ell jb*} V_{\ell E\chi^0}^{LKib} \quad D_2(m^2_{\chi_i^0}, m^2_{\chi_j^0}, m^2_{U_a}, m^2_{E_b}) \\
\left(C_{LR}^{V\Box}\right)_{\chi^0} &= \frac{1}{4}\sum_{i,j=1}^{4}\sum_{a,b=1}^{3} V_{dD\chi^0}^{LJia*} V_{dD\chi^0}^{LIja} V_{\ell E\chi^0}^{R\ell ib*} V_{\ell E\chi^0}^{RKjb} \quad D_2(m^2_{\chi_i^0}, m^2_{\chi_j^0}, m^2_{U_a}, m^2_{E_b}) \\
&\quad + \frac{1}{4}\sum_{i,j=1}^{4}\sum_{a,b=1}^{3} V_{dD\chi^0}^{LJia*} V_{dD\chi^0}^{RIja} V_{\ell E\chi^0}^{R\ell jb*} V_{\ell E\chi^0}^{LKib} \quad D_2(m^2_{\chi_i^0}, m^2_{\chi_j^0}, m^2_{U_a}, m^2_{E_b}) \\
\left(C_{LL}^{S\Box}\right)_{\chi^0} &= -\frac{1}{2}\sum_{i,j=1}^{4}\sum_{a,b=1}^{3} V_{dD\chi^0}^{RJia*} V_{dD\chi^0}^{LIja} V_{\ell E\chi^0}^{R\ell ib*} V_{\ell E\chi^0}^{LKjb} m_{\chi_i^0} m_{\chi_j^0} \quad D_0(m^2_{\chi_i^0}, m^2_{\chi_j^0}, m^2_{U_a}, m^2_{E_b}) \\
&\quad + \sum_{i,j=1}^{4}\sum_{a,b=1}^{3} V_{dD\chi^0}^{RJia*} V_{dD\chi^0}^{LIja} V_{\ell E\chi^0}^{R\ell jb*} V_{\ell E\chi^0}^{LKib} m_{\chi_i^0} m_{\chi_j^0} \quad D_0(m^2_{\chi_i^0}, m^2_{\chi_j^0}, m^2_{U_a}, m^2_{E_b}) \\
\left(C_{LR}^{S\Box}\right)_{\chi^0} &= \frac{1}{2}\sum_{i,j=1}^{4}\sum_{a,b=1}^{3} V_{dD\chi^0}^{RJia*} V_{dD\chi^0}^{LIja} V_{\ell E\chi^0}^{L\ell ib*} V_{\ell E\chi^0}^{RKjb} \quad D_2(m^2_{\chi_i^0}, m^2_{\chi_j^0}, m^2_{U_a}, m^2_{E_b}) \\
&\quad + \sum_{i,j=1}^{4}\sum_{a,b=1}^{3} V_{dD\chi^0}^{RJia*} V_{dD\chi^0}^{RIja} V_{\ell E\chi^0}^{L\ell jb*} V_{\ell E\chi^0}^{LKib} m_{\chi_i^0} m_{\chi_j^0} \quad D_0(m^2_{\chi_i^0}, m^2_{\chi_j^0}, m^2_{U_a}, m^2_{E_b}) \\
\left(C_{L}^{T\Box}\right)_{\chi^0} &= \frac{1}{2}\sum_{i,j=1}^{4}\sum_{a,b=1}^{3} V_{dD\chi^0}^{RJia*} V_{dD\chi^0}^{LIja} V_{\ell E\chi^0}^{R\ell ib*} V_{\ell E\chi^0}^{LKjb} m_{\chi_i^0} m_{\chi_j^0} \quad D_0(m^2_{\chi_i^0}, m^2_{\chi_j^0}, m^2_{U_a}, m^2_{E_b})
\end{aligned}
$$

The remaining Wilson coefficients are obtained by swapping $(L \leftrightarrow R)$ in the above equations.

Chargino contributions

The chargino contributions $\left(C_{XY}^{\mathcal{O}\Box}\right)_{\chi^\pm}$ have a similar form as the neutralino contributions with $D \to U$, $E \to N$, $\chi^0 \to \chi^\pm$, and the indices i, j running from 1 to 2. The main difference is that there are no 'crossed fermion' box diagrams. $X, Y \in \{L, R\}$ refer to helicities, while bars refer to the opposite helicity. For example, $\bar{X} = L$ if $X = R$.

$$\left(C_{XY}^{V\Box}\right)_{\chi^\pm} = \frac{1}{4}\sum_{i,j=1}^{2}\sum_{a,b=1}^{3} V_{dU\chi^\pm}^{XJia*} V_{dU\chi^\pm}^{YIja} V_{\ell N\chi^\pm}^{Y\ell jb*} V_{\ell N\chi^\pm}^{XKib} \quad D_2(m^2_{\chi_i^\pm}, m^2_{\chi_j^\pm}, m^2_{U_a}, m^2_{N_b})$$

$$\left(C_{XY}^{S\Box}\right)_{\chi^\pm} = \sum_{i,j=1}^{2}\sum_{a,b=1}^{3} V_{dU\chi^\pm}^{\overline{X}Jia*} V_{dU\chi^\pm}^{YIja} V_{\ell N\chi^\pm}^{\overline{Y}\ell jb*} V_{\ell N\chi^\pm}^{XKib} m_{\chi_i^\pm} m_{\chi_j^\pm} \quad D_0(m^2_{\chi_i^\pm}, m^2_{\chi_j^\pm}, m^2_{U_a}, m^2_{N_b})$$

E.1.2 Z-penguins

$\left(\Delta F_X^{dZ}\right)_i^{IJ}$ are one-loop contributions to the X-handed ($X = L, R$) $\bar{d}^I d^J Z_\mu$ coupling, with a particular contribution labelled by i. The Wilson coefficients for these penguins are derived via

$$C_{XL}^{V\triangleright} = \left(\Delta F_X^{dZ}\right)^{IJ} \cdot \frac{e}{2\sin\theta_W \cos\theta_W} \frac{1}{M_Z^2}(1 - 2\sin^2\theta_W). \tag{E.1}$$

Here we have written the triangle $\triangleright$ to indicate a penguin diagram contribution.

W-boson vertex contributions

$$\left(\Delta F_L^{dZ}\right)_{uWW}^{IJ} = 3\sum_{i=1}^{3} V_{duW}^{LJi*} V_{duW}^{LIi} V_{WWW} \quad C_2(M_W^2, M_W^2, m^2_{u_i})$$

$$\left(\Delta F_L^{dZ}\right)_{Wuu}^{IJ} = \sum_{i,j=1}^{3} V_{duW}^{LJj*} V_{duW}^{LIi} V_{uuZ}^{Lij} \quad C_2(m^2_{u_i}, m^2_{u_j}, M_W^2)$$

$$-2\sum_{i,j}^{3} V_{duW}^{LJj*} V_{duW}^{LIi} V_{uuZ}^{Rij} m_{u_i} m_{u_j} \quad C_0(m^2_{u_i}, m^2_{u_j}, M_W^2)$$

Higgs-W/Goldstone vertex contributions

$$\left(\Delta F_L^{dZ}\right)^{IJ}_{uH^\pm W} = \sum_{i=1}^{3}\sum_{a=2}^{2} V_{duH}^{LJia*} V_{duW}^{LIi} V_{HWZ}^{a} m_{u_i} C \quad C_0(m^2_{H_a^\pm}, m^2_{u_i}, M_W^2)$$

$$\left(\Delta F_L^{dZ}\right)^{IJ}_{uWH^\pm} = \sum_{i=1}^{3}\sum_{a=1}^{2} V_{duW}^{LJi*} V_{duH}^{LIia} V_{HWZ}^{a*} \quad C_0(m^2_{H_a^\pm}, m^2_{u_i}, M_W^2)$$

Higgs vertex contributions

$$\begin{aligned}
\left(\Delta F_L^{dZ}\right)^{IJ}_{H^\pm uu} &= \sum_{i,j=1}^{3}\sum_{a=1}^{2} V_{duH}^{LJja*} V_{duH}^{LIia} V_{uuZ}^{Lij} m_{u_i} m_{u_j} \quad C_0(m^2_{u_i}, m^2_{u_j}, m^2_{H_a}) \\
&\quad + \sum_{i,j=1}^{3}\sum_{a=1}^{2} V_{duH}^{RJja*} V_{duH}^{LIia} V_{uuZ}^{Rij} \quad C_2(m^2_{u_i}, m^2_{u_j}, m^2_{H_a}) \\
\left(\Delta F_R^{dZ}\right)^{IJ}_{H^\pm uu} &= \sum_{i,j=1}^{3}\sum_{a=1}^{2} V_{duH}^{RJja*} V_{duH}^{RIia} V_{uuZ}^{Rij} m_{u_i} m_{u_j} \quad C_0(m^2_{u_i}, m^2_{u_j}, m^2_{H_a}) \\
&\quad + \sum_{i,j=1}^{3}\sum_{a=1}^{2} V_{duH}^{LJja*} V_{duH}^{RIia} V_{uuZ}^{Lij} \quad C_2(m^2_{u_i}, m^2_{u_j}, m^2_{H_a}) \\
\left(\Delta F_L^{dZ}\right)^{IJ}_{uH^\pm H^\pm} &= \frac{1}{2}\sum_{i=1}^{3}\sum_{a,b=1}^{2} V_{duH}^{LJia*} V_{duH}^{LIib} V_{HHZ}^{ab} \quad C_2(m^2_{u_i}, m^2_{H_a}, m^2_{H_b}) \\
\left(\Delta F_R^{dZ}\right)^{IJ}_{uH^\pm H^\pm} &= \frac{1}{2}\sum_{i=1}^{3}\sum_{a,b=1}^{2} V_{duH}^{RJia*} V_{duH}^{RIib} V_{HHZ}^{ab} \quad C_2(m^2_{u_i}, m^2_{H_a}, m^2_{H_b})
\end{aligned}$$

Neutalino vertex contributions

The neutralino contributions, $\left(\Delta F_{L,R}^{dZ}\right)^{IJ}_{D\chi^0\chi^0}$ and $\left(\Delta F_{L,R}^{dZ}\right)^{IJ}_{\chi^0 DD}$, have the same form as the Higgs contributions with $u \to \chi^0$, $H^\pm \to D$, and the indices i, j running from 1 to 4 and the indices a, b running from 1 to 3.

Chargino vertex contributions

The chargino contributions, $(\Delta F^{dZ}_{L,R})^{IJ}_{U\chi^\pm\chi^\pm}$ and $(\Delta F^{dZ}_{L,R})^{IJ}_{\chi^\pm UU}$, have the same form as the Higgs contributions with $u \to \chi^\pm$, $H^\pm \to U$, and the indices i, j running from 1 to 2 and the indices a, b running from 1 to 3.

Gluino vertex contribution

$$(\Delta F^{dZ}_{L})^{IJ}_{\tilde{g}DD} = \frac{1}{2}\sum_{i=1}^{8}\sum_{a,b=1}^{3} V^{LJai*}_{dD\tilde{g}} V^{LIbi}_{dD\tilde{g}} V^{ab}_{DDZ} \quad C_2(m^2_{\tilde{g}_i}, m^2_{D_a}, m^2_{D_b})$$

$$(\Delta F^{dZ}_{R})^{IJ}_{\tilde{g}DD} = \frac{1}{2}\sum_{i=1}^{8}\sum_{a,b=1}^{3} V^{RJai*}_{dD\tilde{g}} V^{RIbi}_{dD\tilde{g}} V^{ab}_{DDZ} \quad C_2(m^2_{\tilde{g}_i}, m^2_{D_a}, m^2_{D_b})$$

E.1.3 d self-energy contributions

For the self-energy contributions we use the notation of [36], highlighted in Figure E.1.

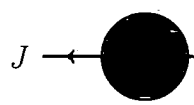

$$= -i\left(\Sigma^q_{VL}\, \not{p} P_L + \Sigma^q_{VR}\, \not{p} P_R + \Sigma^q_{mL} P_L + \Sigma^q_{mR} P_R\right)^{JI}$$

Figure E.1: One-loop threshold corrections to fermion propagators using notation from [36].

W-boson d self-energy contributions

$$(\Sigma^d_{VL})_{uW} = -2\sum_{i=1}^{3} V^{LJi*}_{duW} V^{LIi}_{duW} \quad B_1(0, m_{u_j}, M_W)$$

Higgs d self-energy contributions

$$
\begin{aligned}
\left(\Sigma^d_{VL}\right)_{dH} &= -\sum_{i=1}^{3}\sum_{a=1}^{2} V^{LJia*}_{duH} V^{LIia}_{duH} \quad B_1(0, m_{u_i}, m_{H_a}) \\
\left(\Sigma^d_{mL}\right)_{dH} &= \sum_{i=1}^{3}\sum_{a=1}^{2} V^{RJia*}_{duH} V^{LIia}_{duH} m_{u_i} \quad B_1(0, m_{u_i}, m_{H_a}) \\
\left(\Sigma^d_{VR}\right)_{dH} &= -\sum_{i=1}^{3}\sum_{a=1}^{2} V^{RJia*}_{duH} V^{RIia}_{duH} \quad B_1(0, m_{u_i}, m_{H_a}) \\
\left(\Sigma^d_{mR}\right)_{fs} &= \sum_{i=1}^{3}\sum_{a=1}^{2} V^{LJia*}_{duH} V^{RIia}_{duH} m_{u_i} \quad B_1(0, m_{u_i}, m_{H_a})
\end{aligned}
$$

Neutralino d self-energy contributions

The neutralino contributions to Σ^d have the same form as the Higgs contributions with $u \to \chi^0$, $H^\pm \to D$, and the index i running from 1 to 4 and the index a running from 1 to 3.

Chargino d self-energy contributions

The chargino contributions to Σ^d have the same form as the Higgs contributions with $u \to \chi^\pm$, $H^\pm \to \chi^\pm$, and the index i running from 1 to 2 and the index a running from 1 to 3.

Gluino d self-energy contributions

The gluino contributions to Σ^d have the same form as the Higgs contributions with $u \to \tilde{g}$, $H^\pm \to D$, and the index i running from 1 to 8 and the index a running from 1 to 3.

Colophon

This thesis was made in LaTeX 2_ε using the "hepthesis" class [68], the KDE Integrated LaTeX Environment (Kile) [69] 1.9.1, and the text editing program TextMate [70]. Feynman diagrams were drawn using Jaxodraw [71].

Bibliography

[1] A. Dedes, J. Rosiek, and P. Tanedo, (2008), 0812.4320.

[2] J. (Pseudonym), Resonaances: Ut fit longo magis quam acri bello, World Wide Web electronic publication, 2008.

[3] T.-P. Cheng and L.-F. Li, *Gauge theory of elementary particle physics* (Oxford, 1983).

[4] C. Burgess and G. Moore, *The Standard Mode: A Primer* (Cambridge, 2006).

[5] CKMfitter Group, J. Charles *et al.*, Eur. Phys. J. **C41**, 1 (2005), hep-ph/0406184.

[6] D. Bailin and A. Love, *Supersymmetric Gauge Field Theory and String Theory (Graduate Student Series in Physics)* (Institute of Physics, 1994).

[7] S. P. Martin, (1997), hep-ph/9709356.

[8] J. Rosiek, Phys. Rev. **D41**, 3464 (1990).

[9] J. R. Ellis and D. V. Nanopoulos, Phys. Lett. **B110**, 44 (1982).

[10] S. Dimopoulos and D. W. Sutter, Nucl. Phys. **B452**, 496 (1995), hep-ph/9504415.

[11] Y. Nomura, M. Papucci, and D. Stolarski, Phys. Rev. **D77**, 075006 (2008), 0712.2074.

[12] J. L. Feng, C. G. Lester, Y. Nir, and Y. Shadmi, (2007), 0712.0674.

[13] E. K. Akhmedov, JHEP **09**, 116 (2007), 0706.1216.

[14] K. Lingel, T. Skwarnicki, and J. G. Smith, Ann. Rev. Nucl. Part. Sci. **48**, 253 (1998), hep-ex/9804015.

[15] M. A. Shifman, (1995), hep-ph/9510397.

[16] M. Freeman and L. Jacquet, March of the penguins, 2005.

[17] CDF, T. Aaltonen *et al.*, Phys. Rev. Lett. **100**, 101802 (2008), 0712.1708.

[18] CDF, F. Abe *et al.*, Phys. Rev. Lett. **81**, 5742 (1998).

[19] BaBar, B. Aubert *et al.*, Phys. Rev. **D77**, 032007 (2008), 0712.1516.

[20] HPQCD, A. Gray *et al.*, Phys. Rev. Lett. **95**, 212001 (2005), hep-lat/0507015.

[21] Particle Data Group, W. M. Yao *et al.*, J. Phys. **G33**, 1 (2006).

[22] T. Inami and C. S. Lim, Prog. Theor. Phys. **65**, 297 (1981).

[23] G. Buchalla and A. J. Buras, Nucl. Phys. **B400**, 225 (1993).

[24] J. L. Hewett, S. Nandi, and T. G. Rizzo, Phys. Rev. **D39**, 250 (1989).

[25] X. G. He, T. D. Nguyen, and R. R. Volkas, Phys. Rev. **D38**, 814 (1988).

[26] H. E. Logan and U. Nierste, Nucl. Phys. **B586**, 39 (2000), hep-ph/0004139.

[27] L. J. Hall, R. Rattazzi, and U. Sarid, Phys. Rev. **D50**, 7048 (1994), hep-ph/9306309.

[28] T. Blazek, S. Raby, and S. Pokorski, Phys. Rev. **D52**, 4151 (1995), hep-ph/9504364.

[29] A. Dedes, Mod. Phys. Lett. **A18**, 2627 (2003), hep-ph/0309233.

[30] K. S. Babu and C. F. Kolda, Phys. Rev. Lett. **84**, 228 (2000), hep-ph/9909476.

[31] S. R. Choudhury and N. Gaur, Phys. Lett. **B451**, 86 (1999), hep-ph/9810307.

[32] C.-S. Huang, W. Liao, Q.-S. Yan, and S.-H. Zhu, Phys. Rev. **D63**, 114021 (2001), hep-ph/0006250.

[33] G. L. Kane, C. Kolda, and J. E. Lennon, (2003), hep-ph/0310042.

[34] A. Dedes, H. K. Dreiner, and U. Nierste, Phys. Rev. Lett. **87**, 251804 (2001), hep-ph/0108037.

[35] A. Dedes and A. Pilaftsis, Phys. Rev. **D67**, 015012 (2003), hep-ph/0209306.

[36] A. J. Buras, P. H. Chankowski, J. Rosiek, and L. Slawianowska, Nucl. Phys. **B659**, 3 (2003), hep-ph/0210145.

[37] G. Isidori and A. Retico, JHEP **11**, 001 (2001), hep-ph/0110121.

[38] P. H. Chankowski and L. Slawianowska, Phys. Rev. **D63**, 054012 (2001), hep-ph/0008046.

[39] M. Lenzi, (2007), 0710.5056.

[40] Y. Nomura, M. Papucci, and D. Stolarski, Phys. Rev. **D77**, 075006 (2008), 0712.2074.

[41] J. L. Feng, C. G. Lester, Y. Nir, and Y. Shadmi, (2007), 0712.0674.

[42] H. Dijkstra, (2007), 0708.2665.

[43] H. Georgi, Ann. Rev. Nucl. Part. Sci. **43**, 209 (1993).

[44] G. Buchalla, A. J. Buras, and M. E. Lautenbacher, Rev. Mod. Phys. **68**, 1125 (1996), hep-ph/9512380.

[45] A. J. Buras, (1998), hep-ph/9806471.

[46] C. Bobeth, T. Ewerth, F. Kruger, and J. Urban, Phys. Rev. **D66**, 074021 (2002), hep-ph/0204225.

[47] D. M. Capper, D. R. T. Jones, and P. van Nieuwenhuizen, Nucl. Phys. **B167**, 479 (1980).

[48] S. P. Martin and M. T. Vaughn, Phys. Lett. **B318**, 331 (1993), hep-ph/9308222.

[49] A. Denner, H. Eck, O. Hahn, and J. Kublbeck, Phys. Lett. **B291**, 278 (1992).

[50] A. Denner, H. Eck, O. Hahn, and J. Kublbeck, Nucl. Phys. **B387**, 467 (1992).

[51] J. Rosiek, Production and decays of the mssm neutral higgs bosons in the complete 1-loop diagrammatic approach., World Wide Web electronic publication, 2008.

[52] P. H. Chankowski, S. Pokorski, and J. Rosiek, Nucl. Phys. **B423**, 497 (1994).

[53] A. J. Buras, T. Ewerth, S. Jager, and J. Rosiek, Nucl. Phys. **B714**, 103 (2005), hep-ph/0408142.

[54] F. Gabbiani, E. Gabrielli, A. Masiero, and L. Silvestrini, Nucl. Phys. **B477**, 321 (1996), hep-ph/9604387.

[55] M. Misiak, S. Pokorski, and J. Rosiek, Adv. Ser. Direct. High Energy Phys. **15**, 795 (1998), hep-ph/9703442.

[56] M. Ciuchini *et al.*, JHEP **10**, 008 (1998), hep-ph/9808328.

[57] M. Ciuchini and L. Silvestrini, Phys. Rev. Lett. **97**, 021803 (2006), hep-ph/0603114.

[58] M. Ciuchini, E. Franco, A. Masiero, and L. Silvestrini, Phys. Rev. **D67**, 075016 (2003), hep-ph/0212397.

[59] A. Axelrod, Nucl. Phys. **B209**, 349 (1982).

[60] T. Hahn, (2006), physics/0607103.

[61] C. C. Nishi, Am. J. Phys. **73**, 1160 (2005), hep-ph/0412245.

[62] J. F. Nieves and P. B. Pal, Am. J. Phys. **72**, 1100 (2004), hep-ph/0306087.

[63] S. Pokorski, *Gauge Field Theories (Cambridge Monographs on Mathematical Physics), 2nd ed.* (Cambridge University Press, 2000).

[64] G. Passarino and M. J. G. Veltman, Nucl. Phys. **B160**, 151 (1979).

[65] S. Weinzierl, (2006), hep-ph/0604068.

[66] V. I. Borodulin, R. N. Rogalev, and S. R. Slabospitsky, (1995), hep-ph/9507456.

[67] J. Rosiek, (1995), hep-ph/9511250.

[68] A. Buckley, The hepthesis LaTeXbook class, 2007.

[69] B. P. Jeroen Wijnhout, Holger Danielsson, Kde integrated LaTeX environment, 2006.

[70] Micromates, Textmate: The missing editor, 2008.

[71] D. Binosi and L. Theussl, Jaxodraw: Feynman diagrams with java 1.3-0, 2006.

List of Figures

1.1 Example of a unitarity triangle[5]. 7

1.2 Standard Model contribution to $B - \overline{B}$ mixing. 8

2.1 Illustration of one-loop corrections to the Higgs mass from (a) fermions and (b) scalars. 13

3.1 Heuristic picture of $b \to s$ transitions and the effect of new physics (dashed line). 26

3.2 A penguin diagram, drawn suggestively to look somewhat avian. 27

3.3 One-loop contributions to the H_u coupling with down quarks (a) via Higgsinos and (b) via gluinos which can lead to FCNCs. Flavour indices are suppressed. 31

3.4 Tree-level contribution to $\mathcal{M}_{b\bar{b}-\ell\bar{\ell}}$ in the tree-level mass eigenbasis. The vertices give factors of y_b and y_ℓ respectively. 34

3.5 LHCb sensitivty to $\mathrm{B}_\mathrm{s}^0 \to \mu^+ \mu^-$, adapted from[39]. 36

4.1 Generic box and penguin diagrams contributing to $\mathrm{B}_{\mathrm{s,d}} \to \ell^+ \ell'^-$ with our index and momentum conventions. 40

4.2 Diagrammatic form of the effective operators in equation (4.3). 41

4.3 One-loop gluon diagrams renormalising the effective operators represented in Figure 4.2. 45

4.4 Box diagrams without Majorana fermions. 46

4.5 Box diagrams with Majorana fermions. 47

4.6 1PI Z-penguin diagrams. 47

4.7 FCNC self-energy diagrams. 48

5.1 Low $\tan\beta$ MSSM prediction for $B_s^0 \to \mu^+\mu^-$ vs. LL mass insterion in the d-squark sector, δ^{23}_{dLL}. 52

5.2 Low $\tan\beta$ MSSM prediction for $B_d^0 \to \mu^+\mu^-$ vs. LL mass insterion in the d-squark sector, δ^{13}_{dLL}. 53

E.1 One-loop threshold corrections to fermion propagators using notation from[36]. 78

List of Tables

1.1 Standard Model particle spectrum and quantum numbers. 3

2.1 MSSM superfield spectrum and quantum numbers. 15

2.2 MSSM spectrum after electroweak symmetry breaking. 22

3.1 Properties of the B^0 mesons. 27

3.2 Current experimental bounds and SM expectations for leptonic B decays. 29

5.1 Range of input parameters for parameter space. 51

5.2 Constraints used throughout the MSSM scan 52